Serviço Público Federal
Ministério da Educação
Fundação Universidade Federal de Mato Grosso do Sul

Vinícius Neves Urbanek

INFLUENCE OF INLET MASS FLOW RATE UPON NUTRIENT REMOVAL POTENTIAL FOR DIFFERENT FLOATING TREATMENT ISLAND CONFIGURATIONS IN A STORMWATER POND

Campo Grande, MS
July 2021

Federal University of Mato Grosso do Sul
College of Engineering, Architecture and Urbanism and Geography
Graduation Programme in Environmental Technologies

Vinícius Neves Urbanek

INFLUENCE OF INLET MASS FLOW RATE UPON NUTRIENT REMOVAL POTENTIAL FOR DIFFERENT FLOATING TREATMENT ISLAND CONFIGURATIONS IN A STORMWATER POND

A dissertation submitted in partial fulfillment of the requirements for the Master of Science degree in the Graduation Programme in Environmental Technologies in the Federal University of Mato Grosso do Sul, academic area: *Environmental Sanitation and Water Resources*

Advisors:
Prof. PhD. Johannes Gérson Janzen
Prof. PhD. Manoel Lucas Machado Xavier

Approved in: July 12th, 2021

Dissertation Committee:

Prof. PhD. Fernando Jorge Corrêa Magalhães Filho
UCDB

Eng. PhD. Vinicius Alexandre Sikora de Souza

Campo Grande, MS
July 2021

Abstract

Floating Treatment Islands (FTI) are a relatively new technology, that can be used for water treatment. To evaluate the influence of hydrodynamics over nutrient removal potential of FTI in a stormwater pond, a numerical study was undertaken, evaluating the mass removal under different inlet flow rates and root depths. Simulations were performed using an academic version of the commercial software ANSYS CFX. A brief literature review is presented, to show the main topics studied in the FTI research field, and the gaps that this work aims to fill. Then, numerical studies to evaluate how a Pond+FTI system responds to the variation of inflow under different island positioning configurations are presented. Finally, different root depths under the same inflow condition were tested, to establish a relationship between roots, hydrodynamics and treatment by the FTI. We found that the occurrence of recirculation zones nearest to the FTI favors an enhancement of the fraction of mass entering the root zones, and it is the key hydrodynamic aspect of mass removal by these systems. The systems that performed better presented average velocity between 0.08 and 0.10 m/s inside the pond, with reversed flow patterns in the region of the FTI's roots, conditions that favored both hydraulic residence time and pollutant availability at the root zones. Also, the FTI system presented its best removal performance for relative root depths above 0.45, with an optimal condition being the relative root depth about 0.50, under the perspectives of treatment, hydrodynamics and technical-economic viability.
Keywords: Computational Fluid Dynamics; Floating Treatment Islands; Stormwater Ponds;

Resumo

Ilhas de Tratamento Flutuantes (FTI) são uma tecnologia relativamente nova para tratamento de água. Para avaliar a influência da hidrodinâmica sobre o potencial de remoção de nutrientes de FTI em uma lagoa de detenção, realizou-se um estudo numérico, analisando a remoção de massa para diferentes vazões e profundidades de raízes. As simulações foram feitas com a versão acadêmica do código comercial ANSYS CFX. Uma breve revisão de literatura é apresentada, com os principais tópicos e vazios na literatura que este trabalho deseja preencher. Em seguida são apresentados estudos numéricos para avaliar a resposta de um sistema Lagoa+FTI para a variação de vazão sob diferentes configurações de posicionamento das ilhas. Por fim, diferentes profundidades de raízes foram testadas, para estabelecer uma relação entre as raízes, a hidrodinâmica e o tratamento pelas ilhas. Verificou-se que a ocorrência de zonas de recirculação próximas às FTI favorece um aumento na quantidade de massa adentrando as zonas das raízes, sendo o aspecto chave da remoção de nutrientes por esses sistemas. Os sistemas com melhor performance foram aqueles com velocidades médias na lagoa entre 0,08 e 0,10 m/s, com padrões de recirculação mais próximos às ilhas, favorecendo o tempo de residência e a entrada de poluentes nas zonas de raízes. O sistema de FTI também apresentou as melhores performances para profundidades relativas das raízes acima de 0,45, com uma condição ótima sendo a profundidade relativa das raízes de cerca de 0,50, sob as perspectivas do tratamento, hidrodinâmica e viabilidade técnico-econômica.
Palavras-chave: Fluidodinâmica Computacional; Ilhas de Tratamento Flutuantes; Lagoas de Detenção;

Dedication

I dedicate this work for my beloved parents, Douglas and Vanda.

Declaration

I declare that this dissertation has been composed solely by myself and that it has not been submitted, in whole or in part, in any previous application for a degree. Except where states otherwise by reference or acknowledgment, the work presented is entirely my own.

Vinícius Neves Urbanek

Acknowledgements

First of all, I thank God, for giving me the strength and relief I needed for never giving up on pursuing my objectives. To Him, all Honor and all Glory.

I would like to thank my family, especially my parents, Douglas and Vanda, for providing me support, since the beginning of my studies, and especially during the hardest times I've been through over the last year.

I am grateful to Prof. Johannes Janzen and Manoel Xavier, for their contribution with their knowledge, advices and inspiration over these 5 years that I've been in the CFD laboratory, and for giving me the opportunity to perform this work, in such an interesting research field.

I would also like to thank Manoel again, for his deep contribution and teachings on the model and simulation setup, that made possible for me to run and conclude this work, and my laboratory colleague, Luiz, for helping me so much with the technical part of using SUSE, over the last months. Without their aid, this work would've never been possible.

I would finally like to thank all my colleagues from the laboratory, for all the times we've been working together, drinking lots of coffee and sharing knowledge and life experiences. Every single day of work, study and research was much better with their company.

I also acknowledge the help given by the Universidade Federal de Mato Grosso do Sul (UFMS) and Coordenação de Aperfeiçoamento de Pessoal de Nível Superior (CAPES), with academic support, formation and funding over the years of research.

Funding

This study was financed by the Coordenação de Aperfeiçoamento de Pessoal de Nível Superior – Brasil (CAPES) - Finance Code 001.

This study was financed in part by the Universidade Federal de Mato Grosso do Sul - UFMS/MEC - Brazil.

Contents

List of Figures

List of Tables

Chapter 1

Introduction

In this chapter, the main topic of this dissertation is presented, with background from the literature. The most relevant questions about the subject of this research are discussed, and then objectives are pointed out. The chapter ends briefly describing the structure of the dissertation.

1.1 Background and Motivation

Urbanization can be considered one of the main causes to a number of water quality issues, as mentioned in several studies over the past decades. Characklis and Wiesner (1997) studied the presence of metals and particles in stormwater runoff from an urban watershed, and showed that large amounts of contaminants can be found in urban environments. Other studies have shown similar conclusions regarding other issues, such as biodiversity (POMPEU; ALVES; CALLISTO, 2005; LUO et al., 2017; WANG et al., 2020), water shortages (SRINIVASAN et al., 2013), sub-surface water quality (ENI et al., 2011) and river water quality and pollution (OUYANG; ZHU; KUANG, 2006; REN; CUI; SUN, 2014). Efficient urban planning and management of existing urban areas and, especially, management of water bodies located within these areas become matters of great importance for balancing urban development and water quality, as well as for preservation of the environment and ecosystem services.

In this context, the use of wetlands can be considered an effective tool to improve water quality, controlling pollution from urban stormwater and wastewater (BRIX, 1994). One advantage from wetlands is that they provide diverse ecosystem services such as flood protection, carbon storage, habitat for biodiversity, recreation, and aesthetic value, besides the water treatment itself, as pointed by Guzmán, Nepf, and Berger (2018).

Vymazal (2011) mentions that the first experiments on the use of wetland plants to treat wastewaters dates back from the early 50's, and the information about constructed wetlands began to spread slowly during the 70's and 80's. Hoeger (1988) has made one of the first reports on the application of Floating Treatment Islands, which are sometimes referred as Floating Treatment Wetlands. Terminology about this water treatment system is varied, Bi et al. (2019) mentions at least 12 different names for this kind of system. In this work, it will be referred to as Floating Treatment Islands only, or abbreviated to FTI. Figure 1.1 shows an application of a FTI on a lake in Canada.

Figure 1.1: Floating Treatment Island application in Canada. Source: IISD - International Institute for Sustainable Development (2018)

Both Constructed Wetlands and FTI systems operate similarly, performing water treatment by a complex relation between physical, chemical and biological mechanisms such as filtering, sediment deposition and pollutant uptake by the plants (YEH; YEH; CHANG, 2015; VYMAZAL et al., 1998; VYMAZAL, 2007). Literature about Floating Treatment Islands usually classifies them as variants of Constructed Wetlands, which are made by man, differently from Natural Wetlands (VYMAZAL, 2007, 2011; PAVLINERI; SKOULIKIDIS; TSIHRINTZIS, 2017). The usual components of a FTI system are the plants, the biofilm and a buoyant structure. The plants are usually rooted emergent macrophytes, and are the key factor for water treatment (BI et al., 2019). Factors related to the plants include: root height, growth media, percent of vegetation coverage, methods for buoyancy and the plant species (PAVLINERI; SKOULIKIDIS; TSIHRINTZIS, 2017). Roots also provide a living surface for the development of biofilm, which is another important contributing factor to nutrient removal (STOTTMEISTER et al., 2003; ZHANG et al., 2014).

A basic scheme representing the structure of a FTI is shown in Figure 1.2. Vegetation is attached to a buoyant structure which must allow the growth of the plants, and to support natural buoyancy from the plant roots (CHEN; CUERVO, et al., 2016) or provide it artificially (HEADLEY; TANNER, 2006). As vegetation emerges above the structure, above the water level, the plant roots grow and develop under water. The roots play an important role in treatment, being directly in contact with the water column (PAVAN; BRESCHIGLIARO; BORIN, 2015) serving as a filter to the floating particles, and absorbing nutrients for the plants, despite the contribution of phyto-uptake in overall removal still being a controversial topic about its significance (PAVLINERI; SKOULIKIDIS; TSIHRINTZIS, 2017).

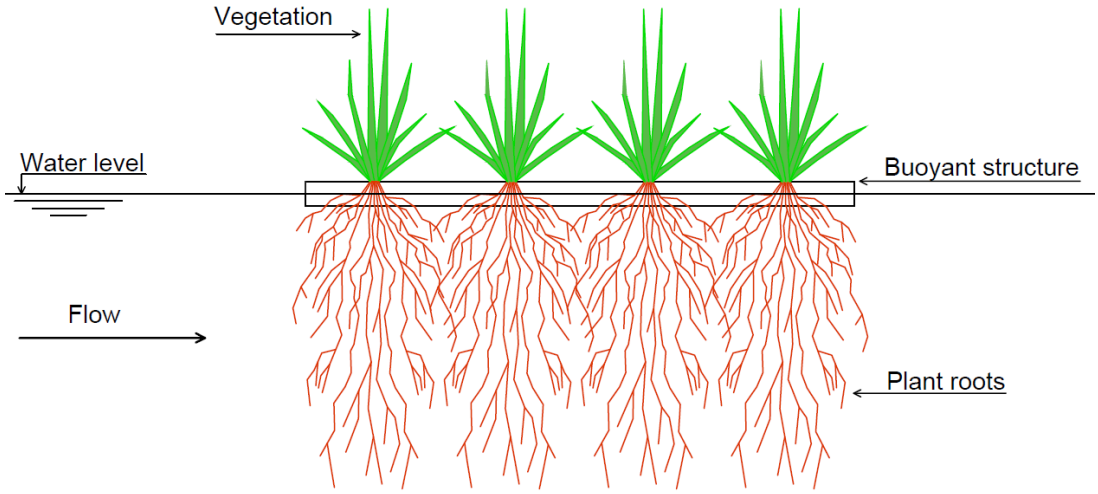

Figure 1.2: Scheme of a Floating Treatment Island structure

In the following topic, considerations about the application of FTI in stormwater ponds are presented.

1.2 FTIs and Stormwater Ponds

Stormwater ponds are constructed structures designed to attenuate peak flow occurred during intense rainfall events, preventing flooding of the downstream basins and reducing erosion risk, besides providing some water quality improvement (HEADLEY; TANNER, 2006). As their primary objective is to slow down the flow from runoff, it results in favoring sedimentation processes inside the pond, therefore, it can be helpful for water treatment, since some operating conditions are met, such as hydraulic performance and the characteristics of the pollutants (MARSALEK; MARSALEK, 1997; WALKER, 1998). The best performance is usually related to hydraulic parameters such as residence time, short-circuiting and mixing, and recent research has been undertaken to evaluate

the efficiency of employing Floating Treatment Islands to maximize the hydraulic performance of stormwater ponds, combining both strategies for water treatment (HEADLEY; TANNER, 2012; KHAN; MELVILLE; SHAMSELDIN, 2013; KHAN; SHOAIB, et al., 2019).

To reduce short-circuiting at stormwater ponds, thus improving their hydraulic performance, the placement of a subsurface berm or an island, in front of the inlet, has shown to be an effective solution (PERSSON, 2000). Guzmán, Cohen, et al. (2018) performed a series of tracer experiments with diverse island topographies for a representative model of a stormwater pond, to assess the ideal configuration for positioning the islands to improve hydraulic performance. They concluded that, besides improving performance, islands positioned within ponds can also contribute for ecology and habitat diversity.

In order to get a deeper knowledge about pond hydraulics and its optimization, Khan, Melville, and Shamseldin (2013) have shown that Floating Treatment Islands can be an effective option to maximize residence time within the pond and reduce short-circuiting: their paper compared results from a model stormwater pond without FTI and with different island configurations. The ones containing FTIs have shown to be more efficient, and this efficiency can be higher or lower, depending on the positioning of the islands. The concentration peak of Residence Time Distribution (RTD) curves tends to appear later in the cases of ponds containing FTI than in a pond without FTI (KHAN; MELVILLE; SHAMSELDIN, 2013; KHAN, 2012; GUZMÁN; COHEN, et al., 2018). Lucke, Walker, and Beecham (2019) reviewed field-based applications of FTIs and concluded that understanding the pond hydraulics and designing it under efficient FTI configurations has a deeper impact on pond performance than simply increasing coverage area.

Besides the hydraulic improvement given by FTIs, the treatment is also enhanced due to the presence of plants, that help with roots serving as filters to entrap and settle particles, helping on sedimentation, with plant roots playing a minor role on nutrient removal by direct uptake, and being also important for biological degradation processes (HEADLEY; TANNER, 2006; SONG et al., 2009). Their importance for aquatic ecosystems is also noted: with a proper coverage of the water surface, they help to improve water quality, reduce algal blooms and absorbing nutrients, being useful for reservoirs, lakes and ponds with significant water fluctuation (NAKAMURA; MUELLER, 2008).

The majority of studies about FTIs within stormwater ponds evaluate water quality and treatment aspects or, most recently and especially after Khan, Melville and Shamseldin (2013), hydraulic aspects such as nominal residence time, short-circuiting, mixing, and general mass flow balances between inlet and outlet. However, Machado Xavier,

Janzen, and Nepf (2018) undertook a study on the hydrodynamics of FTIs analyzing mass removal potential within individual root zones, employing Computational Fluid Dynamics (CFD) techniques to study the flow through FTI's zones and analyze how the islands configuration (geometrical positioning at the pond) impacted on nutrient removal potential. They concluded that a higher removal was achieved by those FTIs with the highest flow rate within the root zone, and the segmentation of an island in multiple islands reduced the removal. Their results also shown a higher mass removal by parallel arrangements, for the scaled model employed. It represented a new approach with potential for the analysis of FTI systems, since it is not only focused in biochemical or hydraulic parameters, but it was able to correlate the islands' configuration with the nutrient removal potential, under a hydrodynamic perspective, giving new possibilities to a deeper understanding of FTI systems' behavior. This work aims to explore these possibilities and expand the results of Machado Xavier, Janzen, and Nepf (2018).

Mass removal by FTI's is controlled by the magnitude of flow through the roots, with the higher values proven to be achieved by FTI's with the highest flow passing through the root zone (HEADLEY; TANNER, 2012; MACHADO XAVIER; JANZEN; NEPF, 2018). However, it is still necessary a better understanding on how this could be affected by different flow rates (within operational flow range) entering the pond. Also, roots are a key factor for this analysis, because they can catch more or less pollutants from water, according to their length. Experiments were undertaken by Khan, Shoaib, et al. (2019) to evaluate influence from roots over treatment, analyzing hydraulic parameters, but a study on the impact of root characteristics on mass removal by individual FTI's is still lacking. Chen, Cuervo, et al. (2016) mention that there is still no detailed and validated design basis for this treatment system to achieve their pollutant removal goals. This work aims to contribute for a better understanding of flow conditions affecting the performance of FTI systems, with the main focus being the analysis of hydrodynamics within stormwater ponds with FTI and flow within root zones, specifically regarding nutrient removal potential, evaluating it for different flow rates, tracer amounts and root depths.

1.3 Objectives

The objective of this study is to evaluate the impact of hydrodynamics over nutrient removal potential of Floating Treatment Islands, using Computational Fluid Dynamics (CFD) simulation techniques. It is expected to expand the results previously obtained, for a most complete characterization of the behavior of FTI systems within stormwater ponds, contributing to the determination of guidelines for the design of FTIs, aiming to

optimize its performance regarding nutrient removal.

The specific methodological goals to achieve our general objective are:

1. Evaluate the influence of inlet flow rates over nutrient removal potential, keeping the same amount of pollutants entering the system;

2. Evaluate the influence of inlet flow rates over nutrient removal potential for different amounts of pollutants entering the system;

3. Evaluate the impact of the FTI root depths over hydrodynamics of the system and nutrient removal potential;

1.4 Dissertation Structure

To explain and detail each methodological goal of the study, this dissertation was divided into 4 chapters. Chapter 1 contains an introduction on the subject of the study, discussing some of the literature about Floating Treatment Islands, their relevance for water quality and pollution control, applications within stormwater retention ponds and potential questions to be studied and analyzed. Chapter 2 presents the first paper, showing the development of the study specifically for objectives 1 and 2, focusing on the analysis of the impact of flow characteristics inside the pond over nutrient removal by FTI. Chapter 3 presents a second paper, related specifically to objective 3, with a numerical study analyzing nutrient removal for a range of relative root depths. Finally, conclusions and recommendations are presented and discussed in Chapter 4.

Chapter 2

Numerical Investigation of the Influence of Flow over Mass Removal by Floating Treatment Islands

In this chapter, the first and second specific objectives of the dissertation are presented. The main objective of this topic was to determine the influence of flow parameters such as flow rate and velocity fields within the pond over FTI performance.

2.1 Introduction

Engineering solutions for macro-drainage of stormwater runoff have been subjects of several studies throughout the years, with one well documented strategy being the use of stormwater ponds. A stormwater pond is a hydraulic structure designed to attenuate peak flow from runoff, helping to prevent issues such as erosion, flooding and structural damages for urban zones and its infrastructure due to intense rainfalls. Headley and Tanner (2006) mentions that ponds can also provide some level of water treatment, due to its own nature of slowing down flow velocities, which favors sedimentation processes. Under this perspective, studies have been conducted aiming to improve the hydrodynamics of stormwater ponds, with the goal of ensuring a most efficient water treatment by them (PERSSON, 2000; KHAN; MELVILLE; SHAMSELDIN, 2013; HEADLEY; TANNER, 2012; GUZMÁN; COHEN, et al., 2018; BIRCH; MATTHAI; FAZELI, 2006).

To ensure good water treatment by stormwater ponds, an alternative that has been explored by research recently is the application of Floating Treatment Islands (FTI), also called Floating Treatment Wetlands, as they are basically a variation of Constructed Wet-

lands (VYMAZAL, 2007; PAVLINERI; SKOULIKIDIS; TSIHRINTZIS, 2017; BI et al., 2019). While the majority of studies on the application of FTI are generally researching for water quality or biological aspects (LADISLAS et al., 2013; CHUA et al., 2012), more recently, some works have begun to focus on understanding the hydrodynamics aspects of water treatment by FTI in stormwater ponds.

Khan, Melville, and Shamseldin (2013) have undertaken experimental tracer studies with a scaled model of a stormwater pond, to analyze hydrodynamic aspects of the use of FTI, aiming to set parameters for design and project of those systems combining FTIs and stormwater ponds. Khan, Shoaib, et al. (2019) expanded the results of the previous work, analyzing some root zone characteristics. These works focused mainly in parameters such as short-circuiting and mixing, dealing with measures based on inlet and outlet results. Among the techniques employed to help on a better understanding of the hydraulic of ponds, Computational Fluid Dynamics (CFD) is one of the most efficient, due to its ability to test different parameters, shapes and operating conditions, with a relatively low cost, when compared with experimental approaches (KHAN; MELVILLE; SHAMSELDIN; FISCHER, 2013).

Under this perspective, Machado Xavier, Janzen, and Nepf (2018) presented a new possibility of analysis of FTI systems, applying a numerical model with CFD techniques to explore different aspects of the hydrodynamics of those systems, analyzing how the positioning of the FTIs affected not only the overall mass removal, but also the performance of individual islands. Their work presented an analysis of water treatment potential under a hydrodynamic approach, showing that the FTI positioning inside a pond can not only improve the pond performance, but also the FTI individual performance is affected by the islands' configuration, which is relevant for the systems' design and application.

To explore the hydrodynamic conditions provided by the best performing FTI configurations presented in Machado Xavier, Janzen, and Nepf (2018), this work aims to expand their results, getting a deeper knowledge of the hydrodynamics of FTI within stormwater ponds, with the objective of identifying how the flow conditions within the pond affect the mass removal by the Floating Treatment Islands, employing for that a numerical model for CFD simulations of tracer studies. To assess the relevance of the flow field for water treatment by FTIs, the results were also compared with tested conditions for different tracer concentrations, to analyze how it impacts on the overall and individual FTI performance. Besides, the mean residence time within individual FTIs was estimated, and correlations with flow parameters were determined.

2.2 Methodology

All simulations of this study were done using the academic version of the software ANSYS Workbench - 2020 R2. Limitations of the academic version and its impact on results are discussed later in this topic, when presenting the mesh employed.

2.2.1 Pond and FTI Geometry

The first step of every CFD study is to determine the flow domain, which is represented by a geometry. For the cases studied in this work, the geometry was a full-scale version of those used in Machado Xavier, Janzen, and Nepf (2018), which was based on a real stormwater pond, described by Khan (2012). The pond geometry is rectangular-shaped, with sloping walls, with a 0.50 m/m slope as the four sides. Pond dimensions are: 41 m long, 15 m wide and 2.3 m deep. Within the ponds, islands were positioned in serial and parallel configurations, with the root zone in both cases representing a fraction of approximately 11% of the pond volume. For the serial configuration, the dimensions of length, width and depth were 7.7 m, 6.0 m and 1.05 m, respectively, equal for both islands. For the parallel configuration, both islands had length, width and depth equal to 15 m, 0.3 m and 1.05 m, respectively. Both tested configurations are presented in Figures 2.1 and 2.2.

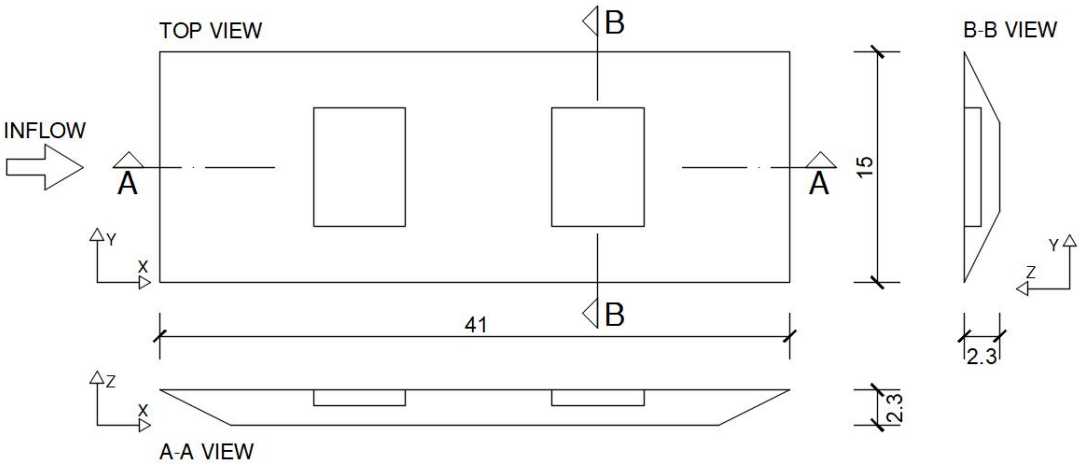

Figure 2.1: Geometry for serial islands configuration. Units in meters.

The system's inlet and outlet boundaries were pipes with diameters of 0.45 m and 1.05 m, respectively. As boundary conditions, it was imposed an uniform flow at the inlet, and a gauge pressure of 0 Pa was specified at the outlet. At the walls, we employed a no-slip boundary condition, and the free-surface flow zone above the pond was set as a symmetry boundary condition, with zero gradient normal to the plane, and no mass

exchange with the pond. The boundary conditions mentioned above are the same applied by Machado Xavier, Janzen, and Nepf (2018), as we employed the same model.

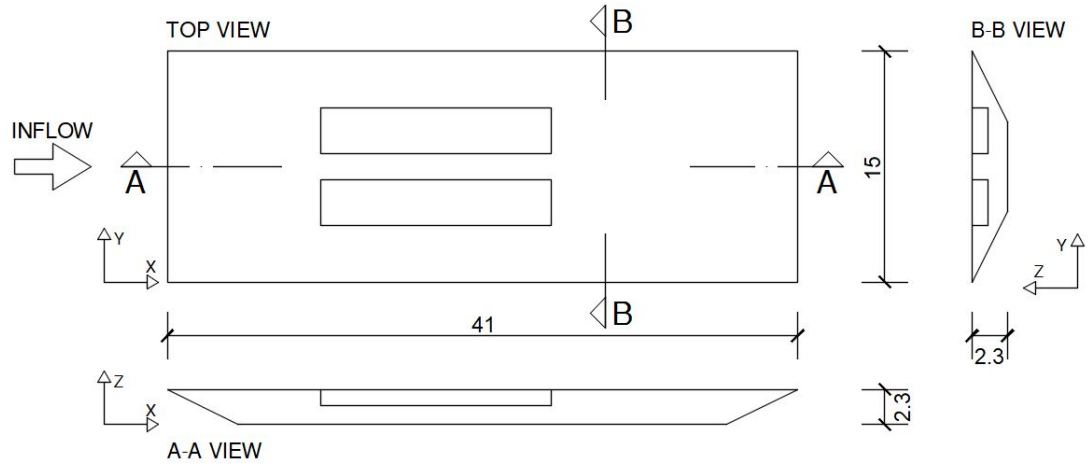

Figure 2.2: Geometry for parallel islands configuration. Units in meters.

2.2.2 Spatial Discretization

Another important step for CFD simulations is the discretization process, by which the flow domain is divided into several smaller elements, and transport equations are solved for each one as a control volume, by the Finite Volumes Method, which is implemented by the numerical code ANSYS CFX Solver. To allow a more accurate representation of the flow boundaries, a unstructured mesh was developed for each geometry. The regions of flow entering or exiting the pond, and also the Floating Treatment Islands and their boundaries were treated with finer mesh sizings.

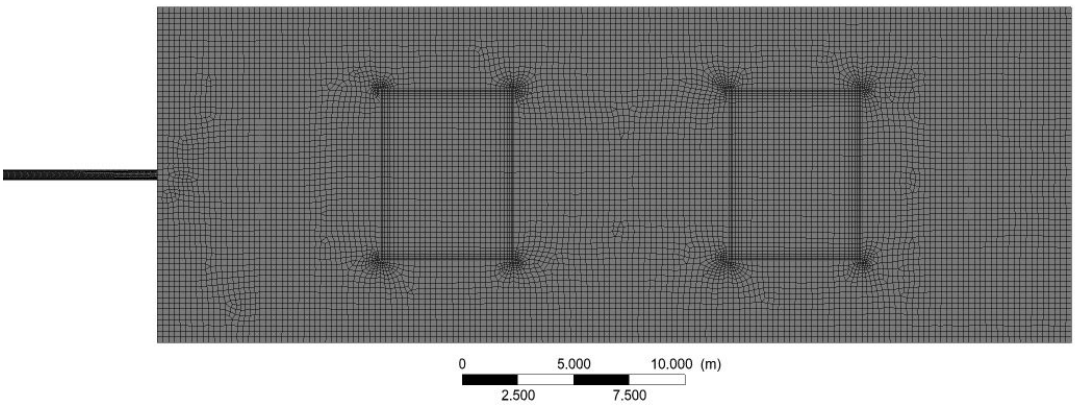

Figure 2.3: Numerical Grid for serial islands configuration

The numerical grid had an approximate number of 10^5 elements. Figures 2.3 and 2.4 show a view from above the numerical grids for both FTI configurations, and it can be noticed that the mesh shows a higher refinement near the FTI's boundaries, as well as

for the inlet pipe. Figure 2.5 shows a detail of the mesh for inlet and outlet pipes, and for a single FTI.

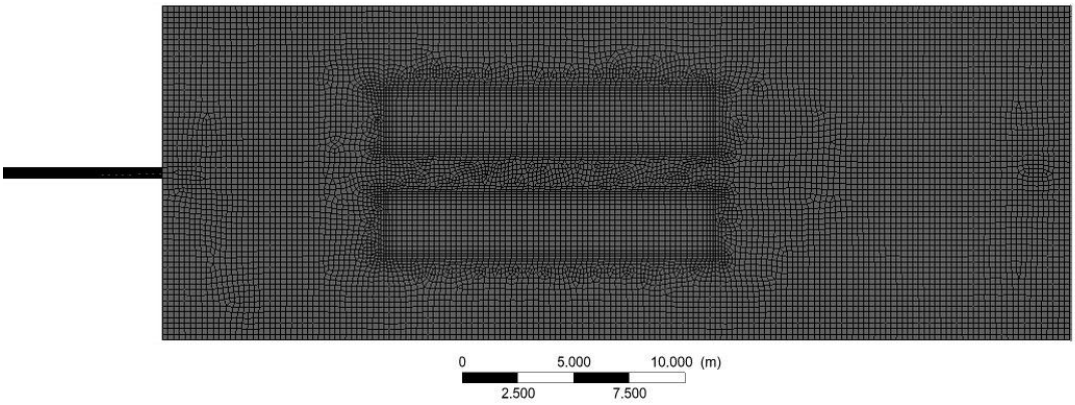

Figure 2.4: Numerical Grid for parallel islands configuration

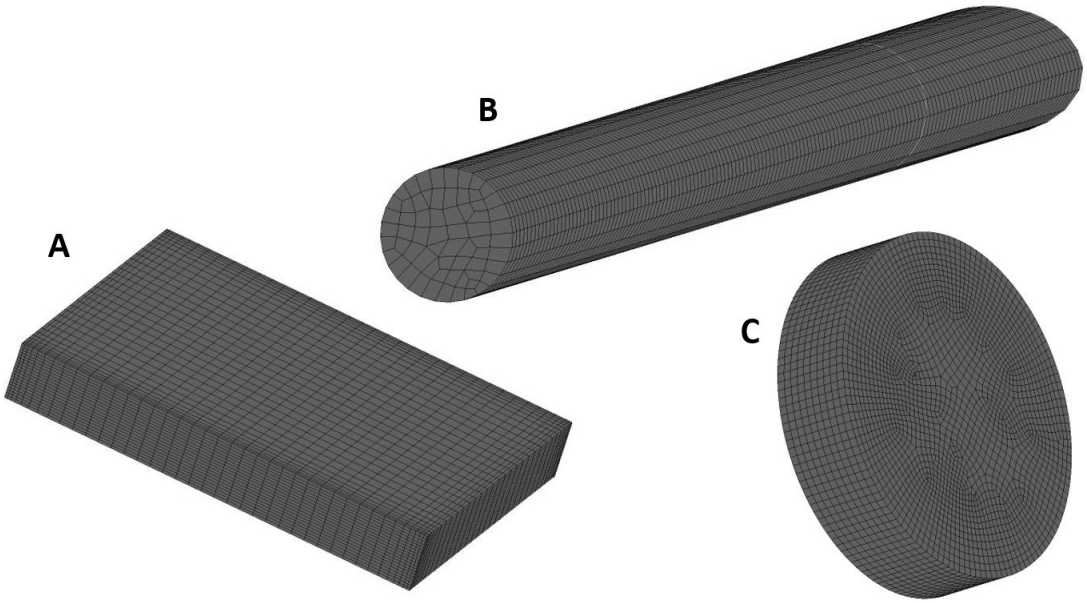

Figure 2.5: Details of the mesh, unscaled. A: Floating Treatment Island for serial cases; B: Inlet pipe; C: Outlet pipe.

2.2.3 Flow Modeling

To determine the flow field within the pond, the CFD code ANSYS CFX 2020 R2 was used. This software is a part of the ANSYS Workbench student version package. Due to the behavior of flow within stormwater ponds, 3D simulations were set, under a transient flow regime. To represent flow turbulence, we employed a Reynolds-Averaged Navier-Stokes (RANS) model, which will be described below. The Reynolds-averaged equations for continuity and momentum are, respectively (ANSYS, 2009):

$$\frac{\partial \rho}{\partial t} + \frac{\partial}{\partial x_i}\left(\rho U_i\right) = 0 \tag{2.1}$$

$$\frac{\partial \rho U_i}{\partial t} + \frac{\partial}{\partial x_j}\left(\rho U_i U_j\right) = -\frac{\partial p}{\partial x_i} + \frac{\partial}{\partial x_j}\left(\tau_{ij} - \rho\overline{u_i u_j}\right) + S_{M,i} \tag{2.2}$$

Where ρ is the fluid density, i,j = 1, 2 or 3, with the indexes 1, 2 and 3, for the x variable, denoting the directions x, y and z (upstream, cross-stream and vertical), respectively; U is the velocity vector, with the indexes corresponding to the velocity components in each direction; τ_{ij} is the molecular stress tensor; $\overline{u_i u_j}$ is the Reynold stress, with u_i being the time varying component of velocity, due to turbulent fluctuations; and $S_{M,i}$ is a momentum source, used to represent the root zone drag.

SST k-omega Turbulence Model

To represent turbulence in the flow, Reynolds stresses and momentum fluxes that appear in the RANS equations need to be modeled, to ensure closure of the problem. In this work, we employed an eddy-viscosity model of 2 equations, the Shear-Stress-Transport (SST) $k-\omega$ model, due its ability to represent flow in both free-stream and boundary layer with good accuracy (MENTER; KUNTZ; LANGTRY, 2003) and relatively low computational effort. On eddy-viscosity models, the momentum equation is slightly modified by adding a term for the effective viscosity:

$$\mu_{eff} = \mu + \mu_t \tag{2.3}$$

Where μ_{eff} is the effective viscosity, μ is the fluid viscosity and μ_t is the eddy viscosity (or turbulent viscosity), which is modelled by the k-ω turbulence model. The momentum equation becomes:

$$\frac{\partial \rho U_i}{\partial t} + \frac{\partial}{\partial x_j}\left(\rho U_i U_j\right) = -\frac{\partial p'}{\partial x_i} + \frac{\partial}{\partial x_j}\left[\mu_{eff}\left(\frac{\partial U_i}{\partial x_j} + \frac{\partial U_j}{\partial x_i}\right)\right] + S_{M,i} \tag{2.4}$$

Where p' is a modified pressure, defined by:

$$p' = p + \frac{2}{3}\rho k + \frac{2}{3}\mu_{eff}\frac{\partial U_k}{\partial x_k} \tag{2.5}$$

Then, the k-ω model assumes that the turbulence viscosity is linked to turbulence kinetic energy (k) and the turbulent frequency (ω) by the relation:

$$\mu_t = \rho\frac{k}{\omega} \tag{2.6}$$

The values for the turbulent kinetic energy and turbulent frequency are calculated by the following equations:

$$\frac{\partial(\rho k)}{\partial t} + \frac{\partial}{\partial x_j}\Big(\rho k U_j\Big) = \frac{\partial}{\partial x_j}\left[(\mu + \sigma_{k2}\mu_t)\frac{\partial k}{\partial x_j}\right] + P_K - \beta^* k\omega \tag{2.7}$$

$$\frac{\partial(\rho\omega)}{\partial t} + \frac{\partial}{\partial x_j}\Big(\rho\omega U_j\Big) = \frac{\partial}{\partial x_j}\left[(\mu + \sigma_\omega \mu_t)\frac{\partial \omega}{\partial x_j}\right] + 2(1-F_1)\sigma_{\omega 2}\frac{1}{\omega}\frac{\partial k}{\partial x_j}\frac{\partial \omega}{\partial x_j} + \alpha\rho S^2 - \beta\rho\omega^2 \tag{2.8}$$

Where S is the strain rate, and the shear production value, P_K is defined as:

$$P_K = min\left[\mu_t \frac{\partial U_i}{\partial x_j}\left(\frac{\partial U_i}{\partial x_j} + \frac{\partial U_j}{\partial x_i}\right), 10\beta^*\rho k\omega\right] \tag{2.9}$$

The advantage of the SST model formulation is the combination of the k-ω model within the inner parts of the boundary layer near the wall, switching to a k-ϵ model in the outer free-stream portion of the flow. To smoothly transition between both formulations, blending functions, F_1 and F_2 are used. The blending function F_1 is:

$$F_1 = tanh(arg_1^4) \tag{2.10}$$

$$arg_1 = min\left[max\left(\frac{\sqrt{k}}{\beta^*\omega d}, \frac{500\nu}{y^2\omega}\right), \frac{4\rho\sigma_{\omega 2}k}{CD_{k\omega}d^2}\right] \tag{2.11}$$

$$CD_{k\omega} = max\left(2\rho\sigma_{\omega 2}\frac{1}{\omega}\frac{\partial k}{\partial x_j}\frac{\partial \omega}{\partial x_i}, 10^{-10}\right) \tag{2.12}$$

The turbulent eddy viscosity, ν_t is defined by the model as:

$$\nu_t = \frac{\mu_t}{\rho} = \frac{\alpha_1 k}{max(a_1\omega, SF_2)} \tag{2.13}$$

$$F_2 = tanh(arg_2^2) \tag{2.14}$$

$$arg_2 = max\left(\frac{2\sqrt{k}}{\beta^*\omega y}, \frac{500\nu}{y^2\omega}\right) \tag{2.15}$$

The SST model coefficients were:

β^*=0.09;

a_1=0.31;

α_1=0.5532, α_2=0.4403;

β_1=0.075, β_2=0.0828;

σ_{k1}=1.176, σ_{k2}=1;

$\sigma_{\omega1}$=0.5, $\sigma_{\omega2}$=0.85616;

Further explanations on the coefficients and the model are found in Menter, Kuntz, and Langtry (2003).

2.2.4 Representing Vegetation as a Porous Zone

In order to represent the FTI's root zone, a porous-media approach was chosen. Treating vegetation as a porous media avoids serious discretization difficulties, due to the complexity of the geometry of the roots. However, this approach also demands careful studies on the permeability coefficient K_{perm}, to guarantee it matches the reality of flow conditions. In this case, permeability was set as $K_{perm} = 10^{-6}\ m^2$, based on a series of tests with different permeability coefficients, selecting the one associated with the best fitting for the velocity field and treatment performance. To model porous media, a momentum source is implemented in ANSYS CFX as a force per unit volume acting on the fluid. The equation for the momentum source in the root zone is shown below:

$$S_{M,i} = \frac{\mu}{K_{perm}} U_i \tag{2.16}$$

To describe the concentration field within the pond and its evolution in the transient simulation, we used the principle of conservation of mass, whose equation is shown below, setting the turbulent Schmidt number, Sc, as 1, which falls into a range of best-fitting measured values described by Gualtieri et al. (2017) for environmental flows.

$$\frac{\partial C}{\partial t} + \frac{\partial (u_i C)}{\partial x_i} = \frac{\partial}{\partial x_i}\left(\frac{v_t}{Sc}\frac{\partial C}{\partial x_i}\right) - k_r C \tag{2.17}$$

$$Sc = \frac{\nu_t}{D_t} \tag{2.18}$$

Where ν_t is the kinematic viscosity, D_t is the turbulent diffusivity, and k_r is the first-order rate constant, which was used to describe mass removal within the root zones as a first-order reaction. In this study, k_r was set as 0.0071, resulting in a non-dimensional removal rate, $k_r t_n$, with t_n being the nominal residence time of the pond, which falls within the range described by Machado Xavier, Janzen, and Nepf (2018) for full-scale ponds, for all tested conditions.

2.2.5 Tracer Studies

To obtain the results, a tracer study was implemented in the CFD code, by adding a new variable to represent the tracer, with same density as water, entering the pond by a 10 s injection. The scaled models from Machado Xavier, Janzen, and Nepf (2018) and Khan, Melville, and Shamseldin (2013) were run with a flow rate at the inlet Q = 1 L/s. To ensure model similarity between different scale models, a Froude number similarity criterion was applied. The equivalent flow rate was calculated by:

$$Q_e = QL_r^{5/2} \tag{2.19}$$

Where Q_e is the equivalent flow rate for the full-scale model, Q is the scaled model flow rate, and L_r is the scale factor. It means that, by that criterion, the equivalent flow rate for the full-scale pond was about 315 L/s. Based on that, we took that flow rate as a control value. The tested flow rates were chosen based on the range mentioned by Khan (2012), which goes from 300 L/s to 500 L/s. Two different situations were considered: in the first, for all inlet flow rates, it was injected the same amount of tracer of the first case of 315 L/s, varying the tracer concentrations at the inlet from about 0.006 kg/m^3 to 0.010 kg/m^3, with higher flow rates receiving a smaller tracer concentration, ensuring that every case had 3.15 g of tracer injected (the same as the control case).

Five different flow rate values at the inlet were tested for each of the FTI configurations. Then, we tested the same inlet flow rates, only for the configuration with the best overall performance, varying the amount mass entering the pond, to evaluate if tracer amount and concentration interferes over the removal performance of FTIs. The tested conditions for all cases are presented in Table 2.1.

The simulation process for each case was divided in 3 main stages. In the first stage, the flow field was determined by a permanent flow regime simulation, without any tracer injection. In the second one, the simulations are set to transient flow, with a time step that goes from 0.1 s at the initial steps, to 10 s at the final steps. In this stage, the

Case	**Island conf.**	Q_{inlet} **(L/s)**	C_{inlet} **(kg/m³)**	$M_{injected}$ **(g)**
1	Serial	315	0.010	31.50
2	Serial	350	0.009	31.50
3	Serial	400	0.008	31.50
4	Serial	450	0.007	31.50
5	Serial	500	0.006	31.50
6	Parallel	315	0.010	31.50
7	Parallel	350	0.009	31.50
8	Parallel	400	0.008	31.50
9	Parallel	450	0.007	31.50
10	Parallel	500	0.006	31.50
11	Serial	350	0.010	35.00
12	Serial	400	0.010	40.00
13	Serial	450	0.010	45.00
14	Serial	500	0.010	50.00
15	Serial	315	0.020	63.00
16	Serial	315	0.016	50.00
17	Serial	315	0.050	157.50
18	Serial	315	0.100	315.00

Table 2.1: Tested conditions of FTI configuration, inlet flow rate, injection concentration and injected mass of the study.

removal term of the islands is set to 0. During the first 10 s, the tracer is injected at the system. Then, the simulation is ran for a time enough to 95% of the tracer mass to exit the pond. Then, for the third stage, the mass removal by FTIs is simulated by enabling the first-order decay expression within the islands, running for the same simulated time that ensured 95% of tracer mass exiting the pond in step 2. For stages 2 and 3, tracer concentration was measured and recorded at the outlet. Considering exit concentration as a function of time, $C_{out}(t)$, we were able to obtain the mass exiting the pond, M_e by integrating the concentration function multiplied by the flow rate:

$$M_e = \int_0^t Q C_{out}(t)\, dt \tag{2.20}$$

The fractional mass removal for the system was calculated as defined by Machado Xavier, Janzen, and Nepf (2018), being 1 minus the ratio of mass leaving the pond to the mass injected.

$$\%M_{removed} = 1 - \frac{M_e}{M} \tag{2.21}$$

It is also of interest to know how each FTI contributes for overall mass removal within a pond. To assess this contribution, extra simulations were run with the decay source enabled for just one island at a time. This was only done by the serial FTI's configuration, due to the greater influence that the upstream island has over flow characteristics and even the tracer quantities that reach the downstream one, which doesn't occur in the parallel case, because of both islands being located side by side. The expression for removal efficiency of an individual FTI, as defined by Machado Xavier, Janzen, and Nepf (2018) is:

$$\%M_{FTI} = \frac{(M_{in} - M_{out})}{M_{in}} \tag{2.22}$$

Where M_{in} is the mass passing the cross-section directly upstream of the FTI, and $Mout$ is the mass passing the cross-section directly downstream of the island. It means that the calculated contribution is relative to the amount of tracer that gets to pass through the cross-section of the island, not by all tracer entering the system. This is important for serial positioning configurations, where part of the mass injected had already been uptaken by the roots of the upstream island.

2.3 Results and Discussion

2.3.1 Hydrodynamics of the Pond and Root Zone

For each island positioning configuration, 5 different flow rates were tested. As will be shown further, when the simulations considering different amounts of tracer entering the pond were undertaken, the velocity fields were basically the same considered in the first series. The velocity fields of both configurations are shown in Figures 2.6 and 2.7 for each inlet flow rate, measured at a plane located at half the width of the pond.

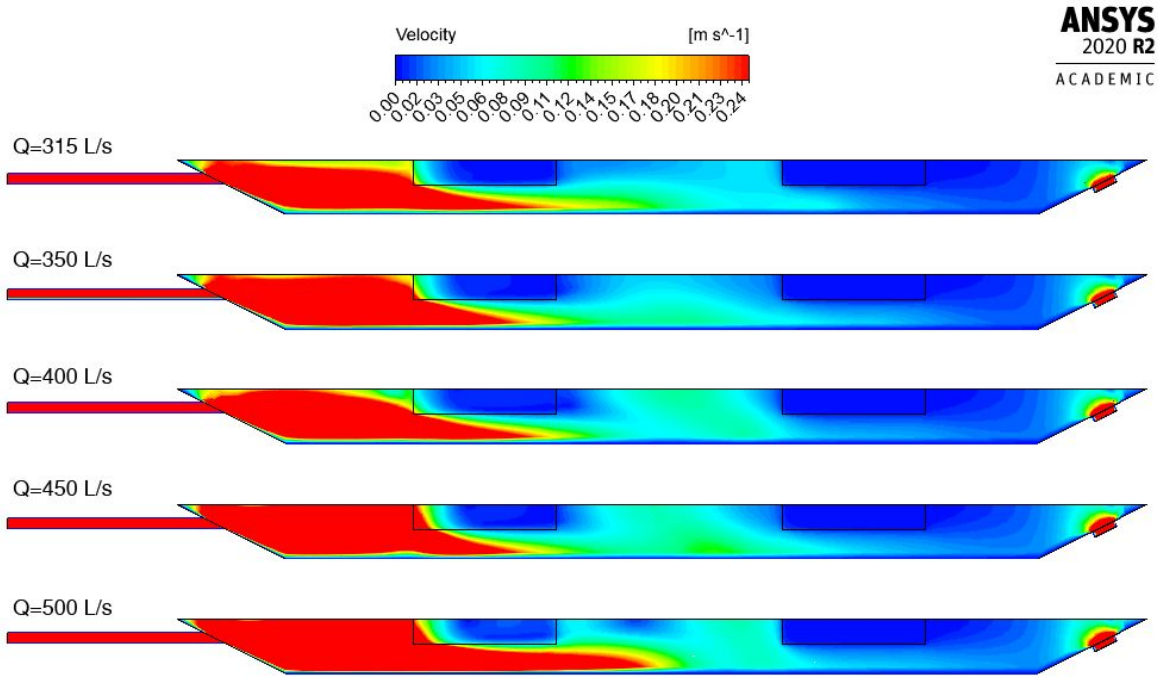

Figure 2.6: Velocity Contours for the pond with FTIs in series.

Analyzing the velocity contours at each positioning configuration, it can be seen that the increase at inlet velocity (i.e. increase at flow rate) leads to an overall situation of higher flow velocities inside the pond. For FTI in series, shown in Figure 2.6 the upstream island presents an obstacle for the flow development, which makes the flow be directed to the bottom part of the pond, showing a zone of flow acceleration below the first FTI. The length of this zone is similar for all cases, with the one with higher flow rate leading to a longer acceleration zone, even reaching the intermediate bottom part of the pond. However, the greater impact this initial acceleration has over the general flow field within the pond is most well seen at the downstream regions, with a higher average velocity profile reaching the second island, which always presents a flow deceleration when compared with the upstream region, due to wakes generated by the upstream FTI (MACHADO XAVIER; JANZEN; NEPF, 2018). Table 2.2 presents the average of the

velocity within the pond and root zones for each case. It is possible to observe that the root zones present great deceleration when compared to the average velocity within the pond. The effects of these aspects over mass removal will be discussed in the following sections.

For the situation of a pond with FTIs in parallel, shown in Figure 2.7, the overall flow velocity inside the pond was also higher for higher inlet flow rates, as it is expected.

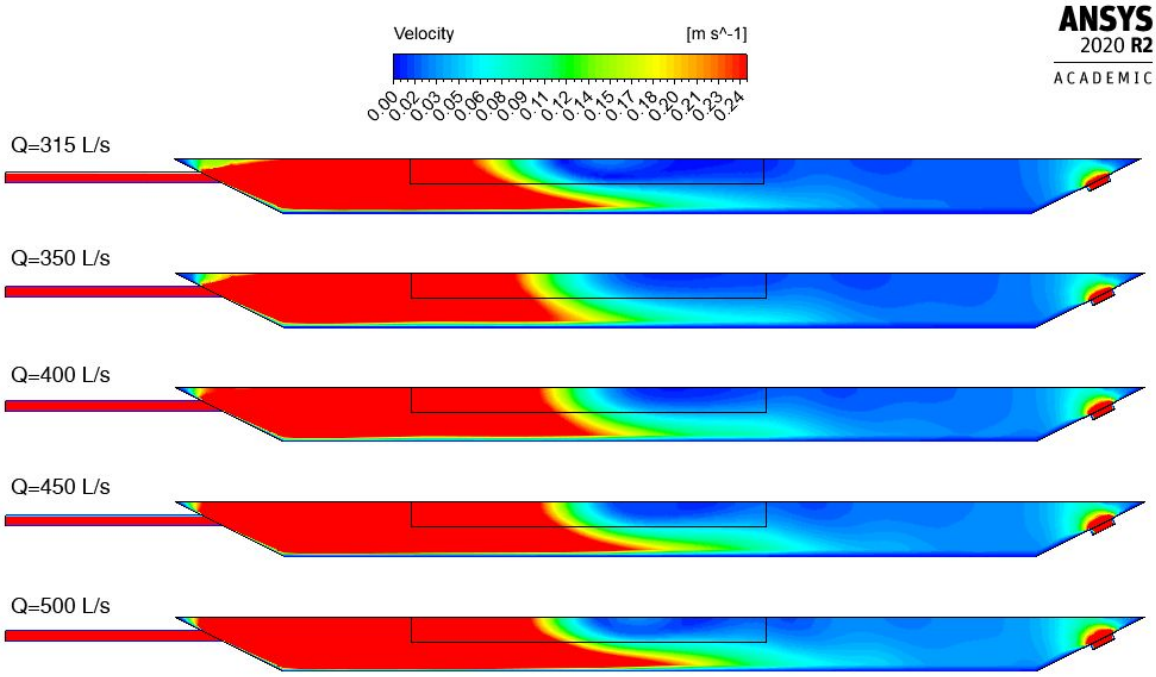

Figure 2.7: Velocity Contours for the pond with FTIs in parallel.

Case	**Island conf.**	Q_{inlet} **(L/s)**	v_{pond} **(m/s)**	v_{FTI1} **(m/s)**	v_{FTI2} **(m/s)**
1	Serial	315	0.083	0.015	6.25×10^{-4}
2	Serial	350	0.085	0.018	6.50×10^{-4}
3	Serial	400	0.111	0.020	7.34×10^{-4}
4	Serial	450	0.108	0.028	9.85×10^{-4}
5	Serial	500	0.130	0.033	1.20×10^{-3}
6	Parallel	315	0.091	0.008	0.009
7	Parallel	350	0.098	0.010	0.011
8	Parallel	400	0.114	0.014	0.014
9	Parallel	450	0.130	0.018	0.017
10	Parallel	500	0.146	0.020	0.021

Table 2.2: Average velocities at the pond and at the root zone of each FTI. v_{FTI1} and v_{FTI2} are the average velocities within the root zones of the upstream and downstream FTI, respectively, for cases 1-5, and for the left and right FTI, for cases 6-10.

However, due to the islands positioning configuration, the space between FTIs leads to an extra acceleration zone, combined with the one below each FTI, which causes higher velocities inside the pond than in the serial case, as can also be seen in Table 2.2. These regions with higher velocity also mean lower pressure zones for the flow inside the pond, which led to different flow patterns caused by flow recirculating, especially in the region between both islands. This difference can be well seen when we analyze the velocity vectors for both FTI positioning configurations.

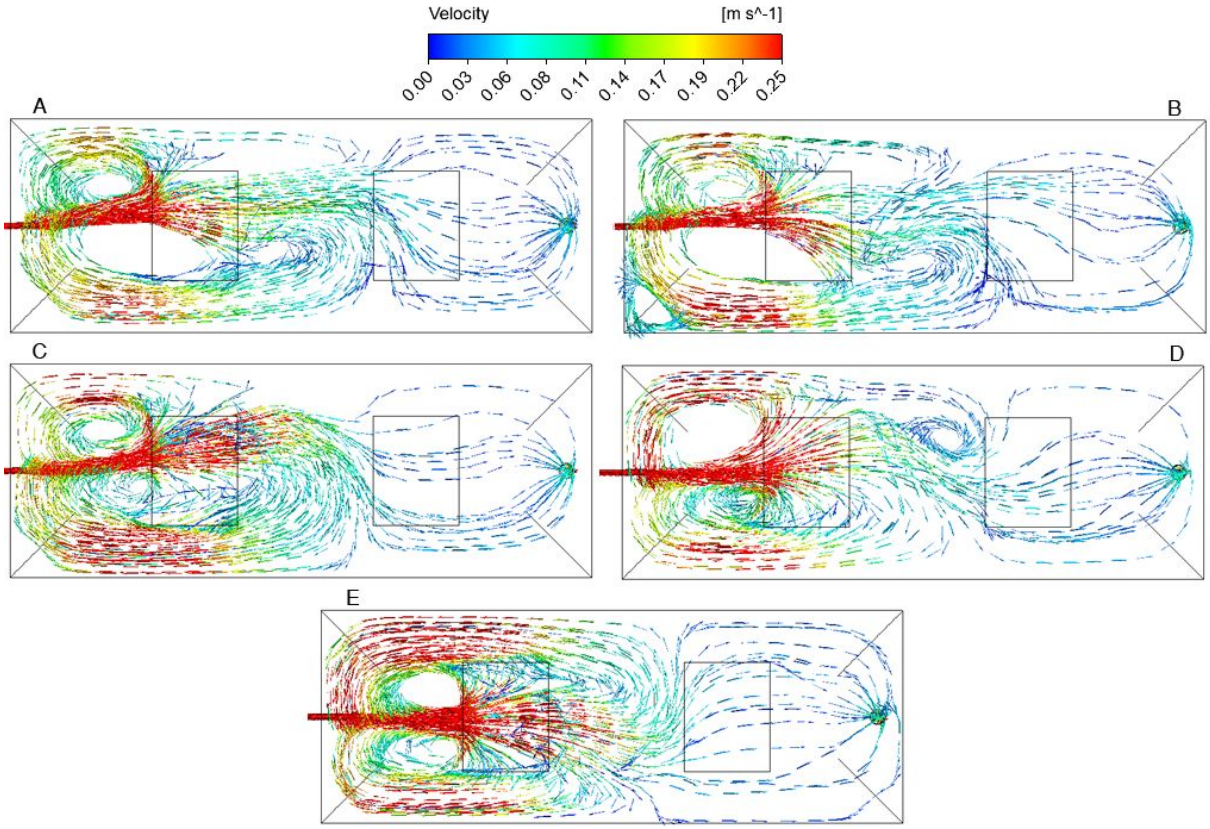

Figure 2.8: Velocity Vectors at the pond with FTIs in series, for inlet flow rates of A: 315 L/s, B: 350 L/s, C: 400 L/s, D: 450 L/s and E: 500 L/s.

Figure 2.8 shows the velocity vectors for the serial configuration. The vectors were generated over equally-spaced streamlines, and give a general idea of how fluid flows throughout the pond and FTIs. Two recirculation zones reach the upstream island, and another two smaller vortices can be noted after flow passes through the bottom of that FTI. For the cases with lower velocities, the second recirculation zone helps bringing fluid back to the root zone of the first FTI, while the flow reaching the downstream island is almost exclusively forward up to the outlet. However, especially at the cases of inlet flow rate of 450 L/s and 500 L/s, that recirculation happens precisely in the intermediate zone between FTIs, which certainly leads to less tracer going backwards and entering the root zone of the upstream FTI.

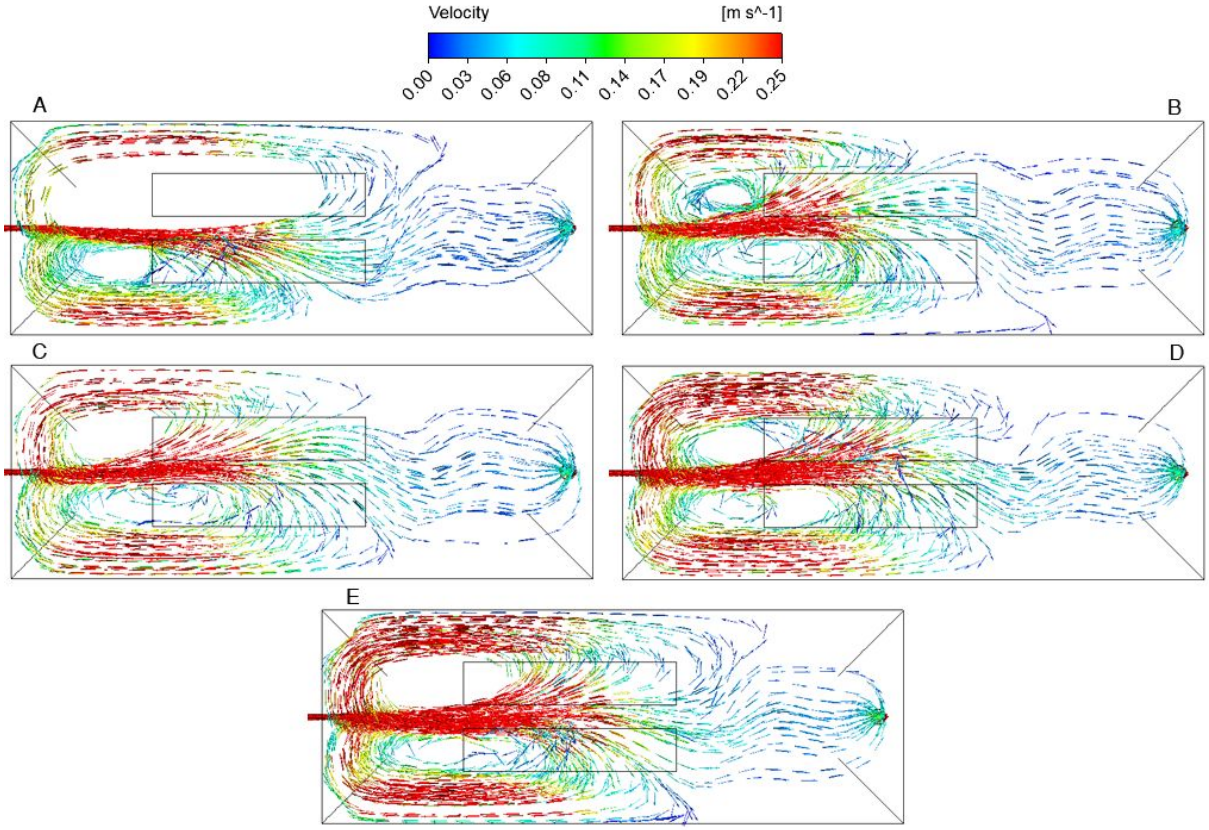

Figure 2.9: Velocity Vectors at the pond with FTIs in parallel, for inlet flow rates of A: 315 L/s, B: 350 L/s, C: 400 L/s, D: 450 L/s and E: 500 L/s.

In the cases of a set of FTIs in parallel within the pond, the recirculation patterns, as shown in Figure 2.9, appear to have only two major vortices, both happening about half the length of the islands, with smaller vortices inside of them at the upstream face of each FTI. An essential difference of the mass uptake by the root zones of parallel islands, when compared to serial configurations, is that there is a large contribution of the islands' sides, while the majority of flow in serial configurations enter by the upstream faces. This recirculation pattern was already expected, due to the locally adverse pressure gradient, as described by Machado Xavier, Janzen, and Nepf (2018). The same work also mentions the relevance of the reversed flow happening inside the pond for a better mass removal performance of the FTI system. However, the increase of velocity between islands also brings negative consequences for water treatment, since it means that a fraction of the tracer entering the pond will leave in a lower interval of time, or will pass through the root zone for a time smaller than the necessary for an efficient mass uptake by the plants, meaning a lower hydraulic residence time. The geometry of the FTI system, similarly to what happens in other types of wetlands, interferes over the treatment, and in this case, the same way as Sabokrouhiyeh et al. (2017) shows that geometric characteristics of wetlands have influence over hydraulic residence time, it also occurs for the case of FTIs.

For both parallel and serial configurations, we analyzed the streamwise velocity through the root zone, to identify zones with flow rate tending to zero and also the points where flow starts to recirculate. Streamwise velocity was normalized by the velocity at the leading edge of the FTI. As expected for cases with flow entering a porous zone, at the upstream FTI, the high drag due to root density leads to deceleration of flow velocity, over a length X_D. This length, as described by Chen, Jiang, and Nepf (2013), is a function of the root zone height. Machado Xavier, Janzen, and Nepf (2018) obtained in their numerical study a relationship of X_D/h=1, where h is the root zone height, for a root zone permeability of 10^{-7} m². However, subsequent studies still not published have shown better results when considering a permeability value of 10^{-6} m², which thus was chosen for the simulations of the present study. Due to that change in permeability, the normalized streamwise velocity results were different in this case. As can be seen from 2.10, the flow velocity consistently tends to reach the value of zero at x/h = 1.5 for all flow rates considered. This higher value can be explained by the higher permeability, which allows more fluid to enter the root zone and reach longer distances inside of it. Beyond the relative distance x/h=1.5, the streamwise velocity inside the roots present reversed flow patterns with slow velocity, which also contributes for mass uptake.

At the downstream FTI of the serial cases, there was no recirculation pattern within the root zone, despite a great deceleration occurred for all cases. Those islands didn't show a reversed flow characteristic such as the FTIs positioned upstream, but their bad hydrodynamics regarding to backflow was slightly compensated by their lower velocities, which allowed the smaller amounts of tracer that reached the FTI to be uptaken by the roots. Figure 2.11 shows the normalized streamwise velocity at the downstream FTI root zone for each flow rate. A similar flow pattern can be seen, with flow velocity almost constant around $U*_{root}$=0.1 through the most part of the root zone, presenting an acceleration tendency as the flow approaches the downstream face of the island. Differently from the upstream FTI, the downstream face do not show reversed flow patterns, which can also explain the lower removal performance achieved by that FTI, since the tracer inflow through the root zone (i.e. pollutant availability for the roots) is reduced when there is no reversed flow tendency (MACHADO XAVIER; JANZEN; NEPF, 2018).

The parallel FTI configuration presents a very different behavior (Fig. 2.12), when compared to the serial configuration. For higher inlet flow rates, the velocities within the root zone presented a small acceleration tendency between x/L = 0.10 and 0.20, after the initial deceleration, followed by another deceleration of the flow, that led to the flow to become reversed. In these cases, the reversed flow tendency only started to appear more clearly after half the length of the FTI. For the other cases, however, the initial tendency was exactly the reversed flow, which was seen for most of the island's length, such as in

Machado Xavier, Janzen, and Nepf (2018). The complexity of the streamwise velocity patterns from each flow rate can be assumed as due to the acceleration zone between both islands, which causes different recirculation zones for each velocity field. However, it still can be noted that the slowest inlet flow rates (315 L/s and 350 L/s) presented the longest region of reversed flow in the x-direction, while the cases with higher flow rates presented less recirculation, and its reversed flow zones appeared later and covering a smaller fraction of the FTI length. The reversed flow tendency had already been noted due the high flow blockage in porous layers and vegetated flow by Rominger and Nepf

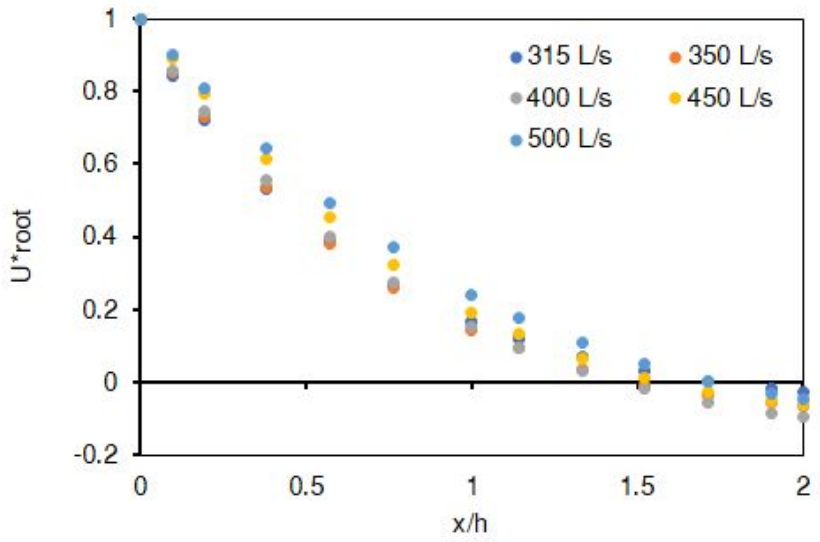

Figure 2.10: Normalized streamwise velocity within the root zone of the upstream FTI for cases with serial configuration. $U*_{root} = U/U_o$, where $U*_{root}$ is the normalized velocity, and U_o is the velocity at the leading edge.

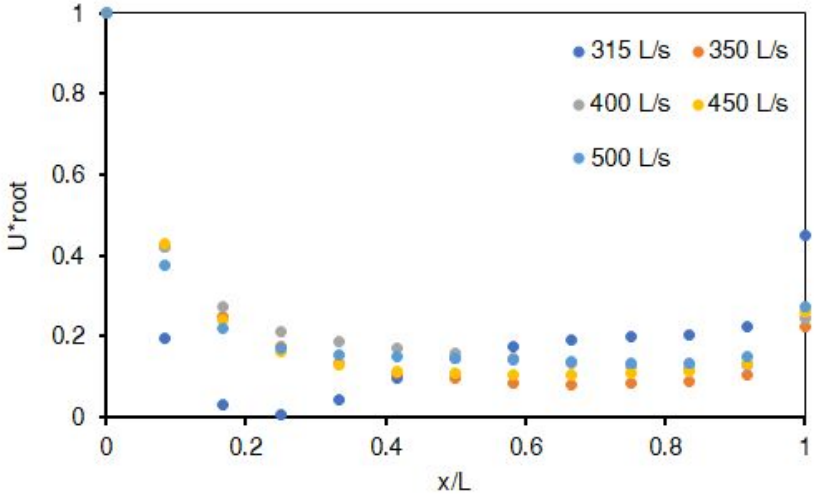

Figure 2.11: Normalized streamwise velocity within the root zone of the downstream FTI for cases with serial configuration. $U*_{root} = U/U_o$, where $U*_{root}$ is the normalized velocity, and U_o is the velocity at the leading edge.

(2011) and Machado Xavier, Janzen, and Nepf (2018).

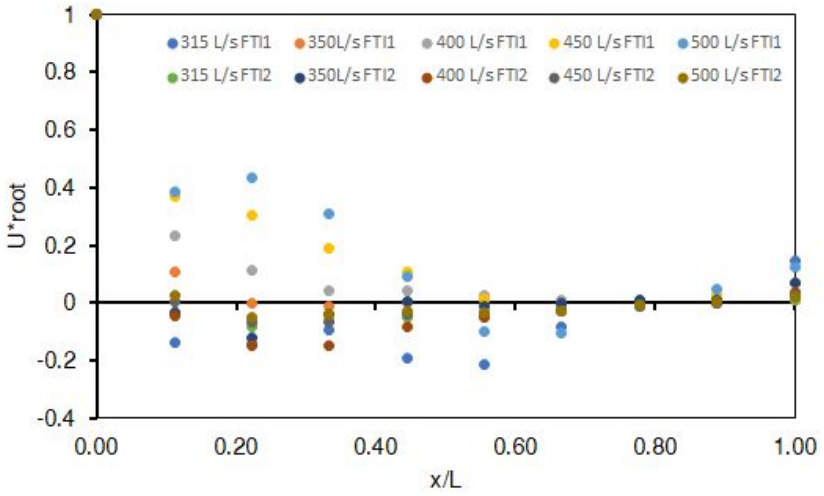

Figure 2.12: Streamwise velocity within the root zone of the FTIs in parallel. $U*_{root} = U/U_o$, where $U*_{root}$ is the normalized velocity, and U_o is the velocity at the leading edge.

2.3.2 Mass Removal of Serial and Parallel configurations

The cases with lower concentrations and higher flow rates were the ones with the lowest mass removal, for both serial and parallel island positioning configurations, as can be seen in Figure 2.13. For the flow rates of 350 L/s and 400 L/s, tracer removal was the same for both configurations. However, FTIs positioned in series showed better performance than FTIs in parallel for the lower and the higher flow rates, which makes the overall performance of the first better than the latter.

We believe that the lower performance of parallel configurations is due its dependency of the flow entering by the inner sides between both islands. Khan, Melville, and Shamseldin (2013) showed that the inlet position at the pond has a considerable influence over the hydrodynamics of ponds, which also affects nutrient removal, and Machado Xavier, Janzen, and Nepf (2018) showed that an island positioning that favors a higher tracer inflow through the roots also benefits its treatment performance. For serial cases, the greatest amount of tracer is captured directly by its upstream faces, which are positioned directly in front of the tracer inflow jet. For FTI in parallel, tracer flows between both islands, and enters the island mainly due to re-circulation in that region. This means that, despite having a larger surface area for the tracer to enter the root zone, there is a larger average distance from inflow, and this might lead to a lesser amount of tracer being captured by parallel islands.

Another result of interest on the research was to understand how hydrodynamics

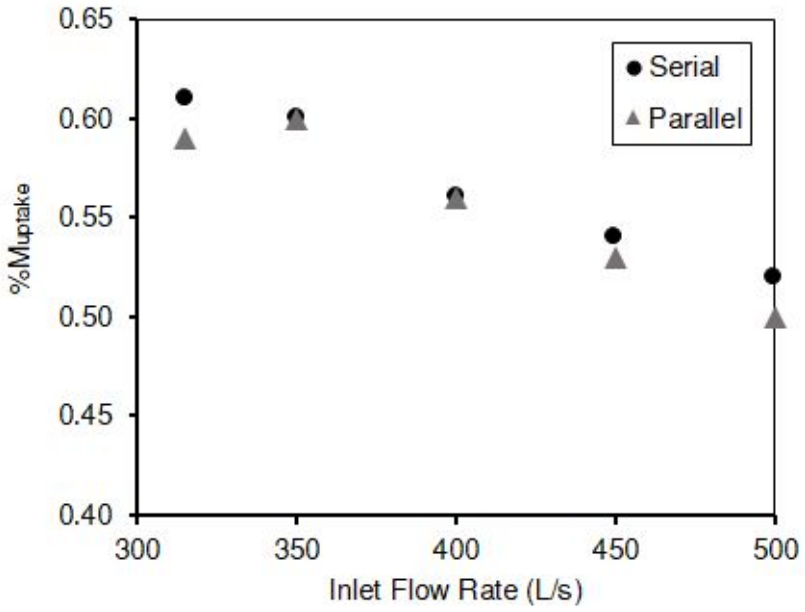

Figure 2.13: Mass removal vs Inlet flow rate. The black dots are the results for FTIs positioned in series, and the grey dots are the results for parallel FTI configuration.

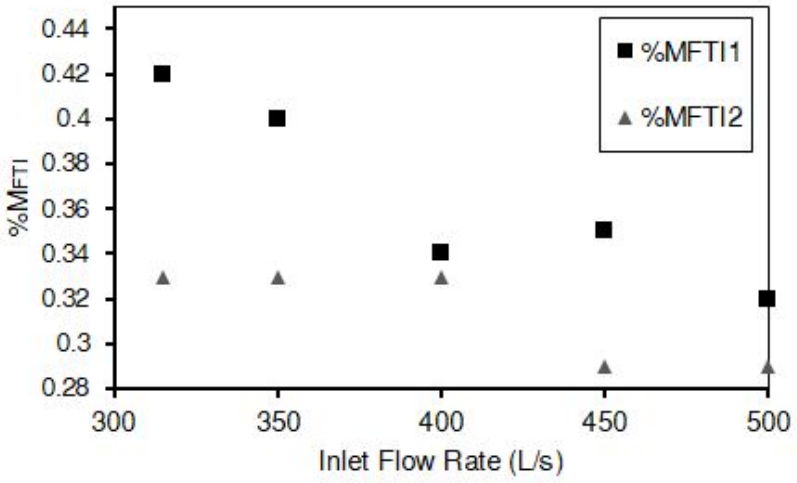

Figure 2.14: Comparison of fractional mass removal vs inlet flow rate for individual FTIs in series.

influence the performance of individual FTIs, especially for the cases with island positioned in series, since the FTIs at a parallel configuration receive similar amounts of tracer, presenting similar hydrodynamics. The island positioned nearest to the inlet, upstream the pond, was called FTI1, and the island positioned downstream the pond, near the exit, was called FTI2. For case 1, which was the control case, both FTI1 and FTI2 performances matched that obtained by the 1:10 scale simulations from Machado Xavier, Janzen, and Nepf (2018), with the upstream island showing a higher fractional mass removal when compared with the one positioned downstream.

Figure 2.14 shows that the fractional mass removal for upstream FTI tends to get worse as inlet flow rate increases, while the downstream FTI presents lower values for higher flow rates, but still close values. The difference between the cases with best and worst performance of FTI1 was 0.10, while for FTI2 this difference was of 0.04. This can be explained by the characteristics of the flow within each FTI's position. FTI1, positioned upstream, receives a higher amount of tracer mass by the jet coming from the inlet, and also has a contribution of reversed flow caused by the recirculation patterns, that might be helpful for the FTI performance when leading to tracer recirculating and entering the root zone, which occurs especially for the cases where the streamwise velocity is lower (i.e., the lower inlet flow rates). In the case of FTI2, the reversed flow is not as present as in FTI1, so the main factor influencing for its removal performance is the amount of mass available for each island to perform its removal (MACHADO XAVIER; JANZEN; NEPF, 2018). The higher inlet flow rate still leads to higher velocities at the downstream FTI, that presents less efficient performances at these conditions when compared to the upstream FTI, since the mass availability generated by the hydrodynamics for that geometrical position is lower.

Case	Q_{inlet} **(l/s)**	$\%M_{uptake}$	$\%M_{FTI1}$	$\%M_{FTI2}$
1	315	0.61	0.42	0.33
2	350	0.60	0.40	0.33
3	400	0.56	0.34	0.33
4	450	0.54	0.35	0.29
5	500	0.52	0.32	0.29
6	315	0.59	-	-
7	350	0.60	-	-
8	400	0.56	-	-
9	450	0.53	-	-
10	500	0.50	-	-

Table 2.3: Mass uptake results for cases with same amount of mass entering the pond.

When we analyze the results, observing the velocity vectors and contours for each serial and parallel case, as presented in the previous topic, the relevance of flow recirculation and tracer retention time within the pond is highlighted. The cases that presented the best mass removal performance were those with smaller velocities (i.e. longer residence times) at the root zone, and with the reversed flow patterns closer to the FTI1, leading to more tracer reaching the roots. This increased tracer availability to the root zones makes the treatment be enhanced (HEADLEY; TANNER, 2012; MACHADO XAVIER; JANZEN; NEPF, 2018). Higher velocities, besides reducing the time that tracer stays within the roots to be uptaken by the decay reaction, also causes the recirculation zones

to occur in the intermediate region between serial islands, or at a longer distance from the FTI leading edge, for parallel cases, causing a higher probability of part of the tracer leaving the pond without passing through the root zones. Mass removal achieved by individual FTIs is presented in Table 2.3.

2.3.3 Residence Time within the Root Zones

Another parameter analyzed by this study was the average tracer concentration at the root zones of each FTI. The CFD techniques make possible to calculate the average tracer concentration over time at the islands, which generated something similar to a RTD curve. The concentration was normalized by C_o, which is defined as the total mass entering the pond, M, divided by the pond volume, V. As shown in Figure 2.15, the ideal plug flow situation within a pond is affected by mixing and short-circuiting. In this work, we will assume that these considerations can be valid when analyzing the residence time within a single FTI root zone.

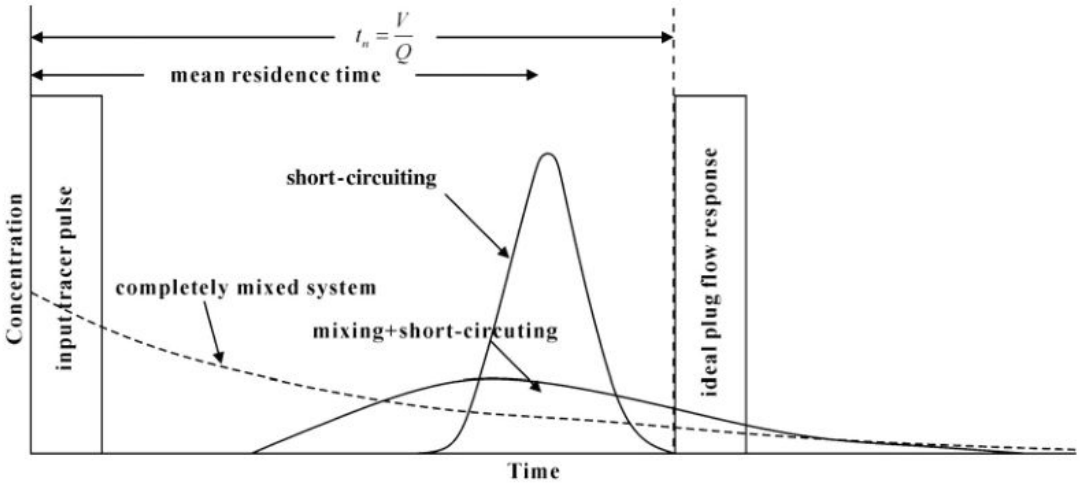

Figure 2.15: Ideal plug flow and completely mixed flow; short-circuiting reduces travel time while mixing attenuates response at outlet. (KHAN; MELVILLE; SHAMSELDIN, 2013)

Analyzing the behavior of the upstream FTI, Figure 2.16 shows the normalized concentration over time in a logarithmic scale, to make possible to see the behavior of the curves at the initial seconds. As can be seen from the curves, the case with the higher peak value of $C*$ is the one with the lower fractional mass removal. The curves for the inlet flow rates between 400-500 L/s show a shape closer to the shape of a situation of short-circuiting, even in logarithmic scale, while the other two cases present a different shape. What can be inferred is that the cases of Q_{inlet} = 315 L/s and 350 L/s are the ones with the peak shape less closer to a single pulse, and keep a relatively high value for a longer

interval of time, reaching values slightly greater than the others after the concentration starts to decrease. We believe that this prolonged peak may have a relevant role on the mass uptake by the upstream island under lower velocities, since it means that a larger amount of tracer is retained within the root zone for a longer time, which makes the decay reaction perform a higher uptake. When analyzing the parallel FTI configuration, Figure 2.18 shows the average concentration at the pair of islands. We can see that the values of $C*$ are lower for the parallel case than in the serial upstream island, that has the same volume as each island of the parallel configuration. The shape of the curves also appears to be closer to the one representing a short-circuiting situation, with short peaks and a narrow shape. This behavior can also explain the weakest performance of a pond with FTIs in parallel when compared to one with FTIs in series.

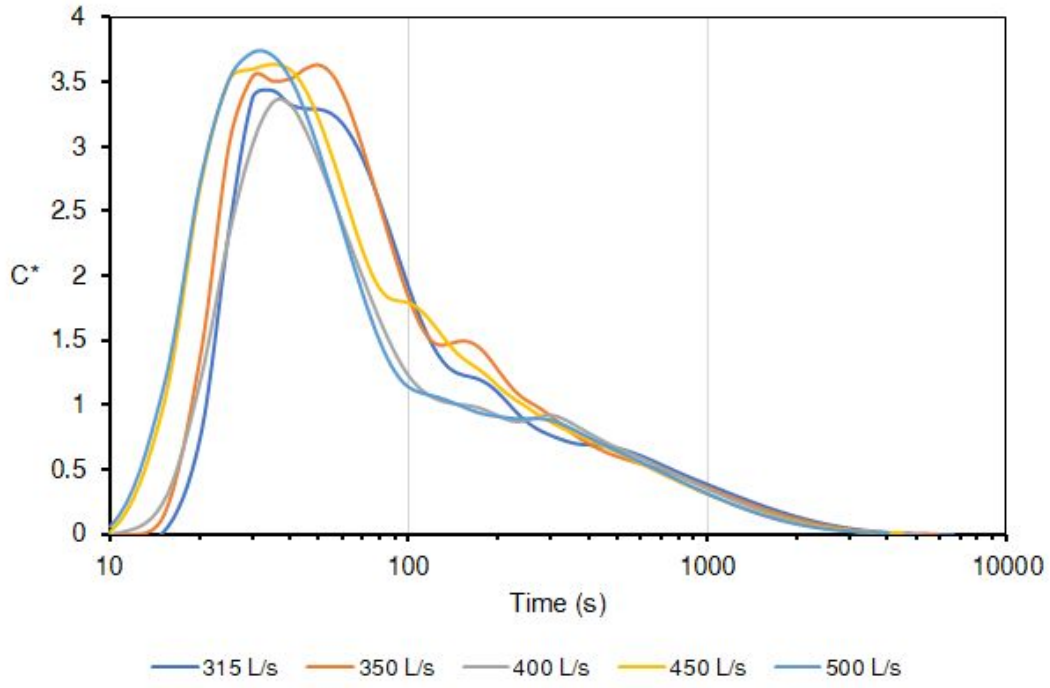

Figure 2.16: Normalized Average Concentration, C*, at the upstream FTI, for the cases with serial FTI configuration.

At the downstream FTI, as shown in Figure 2.17, tracer starts to appear at the root zone between 80 s and 140 s, and the residence time curve presents a heavy increase in tracer concentration at the initial seconds, resulting in a more attenuated decreasing nature. Their peaks are much lower than the peaks of the upstream islands, and their curves show a mixing pattern, with a slower decrease in concentration, resulting in a higher mean residence time (Table 2.4). However, despite having a higher mean residence time compared to the upstream FTI, their mass removal is still lower. It could be explained due to a smaller mass availability for the downstream FTI, caused by the velocity fields in that region of the pond, which has shown to be a limiting factor for mass removal. The residence time is still relevant when we compare the removal by the downstream FTI

under different inlet flow rates, with the individual removal being higher for the cases presenting the higher residence times.

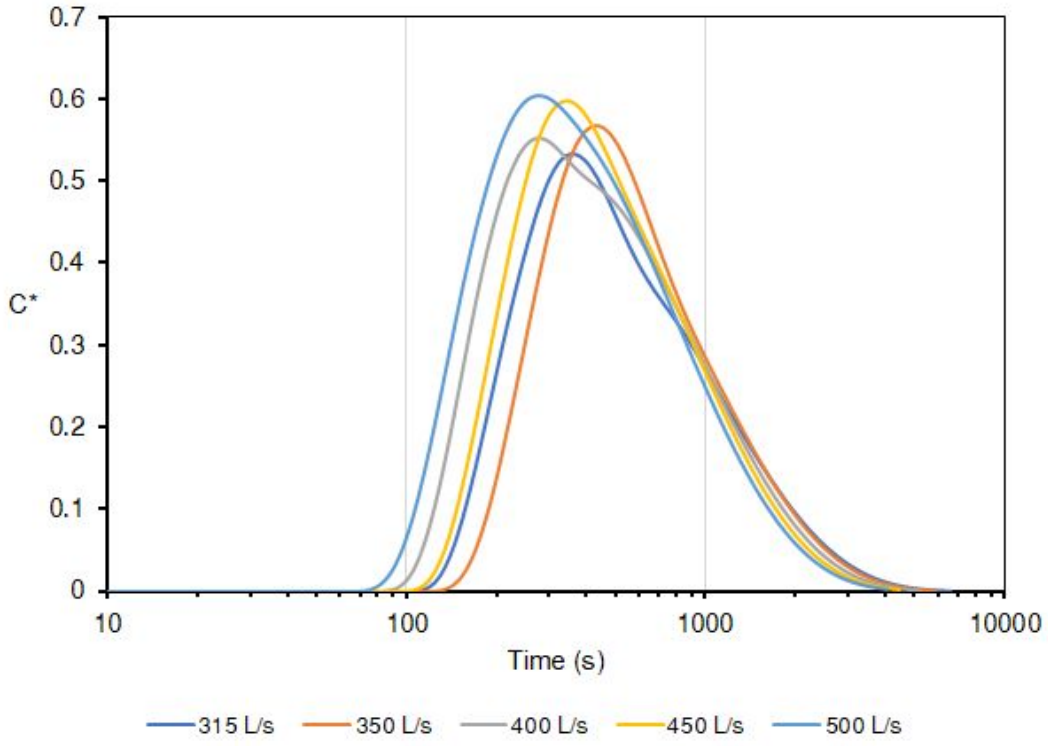

Figure 2.17: Normalized Average Concentration, C*, at the downstream FTI, for the cases with serial FTI configuration.

Besides identifying the concentration patterns along the time within each FTI, it was also possible to estimate the mean residence time, t_{mean} of each island. The mean residence time of a particle of tracer within an FTI was estimated by the expression:

$$t_{mean} = \frac{\int_0^\infty tCdt}{\int_0^\infty Cdt} \tag{2.23}$$

The calculated values of t_{mean} for each FTI of the serial case are shown in Table 2.4, with t_{mean1} and t_{mean2} being the mean residence times for the upstream and downstream FTI, respectively. The values of t_{mean2} were higher than the values of t_{mean1}, due to the island's position and lower flow velocities, which made the tracer remain for longer intervals of time. However, their residence time distribution has indicated that the flow reaching the downstream FTI had already been mixed, with tracer concentrations being always lower than in the upstream islands. Asides for that, when we analyze the average mean residence time of the pair of FTI, $\bar{t}_{mean}$, and compare it to the average value of the parallel configuration, it is possible to see that the increase in the residence time within FTIs is associated with lower velocities and more favorable recirculation, generating an increase of the mass uptake by the roots, which corroborates the proposed hypothesis,

that the hydrodynamics of flow inside the pond is directly responsible for a FTI's mass removal performance.

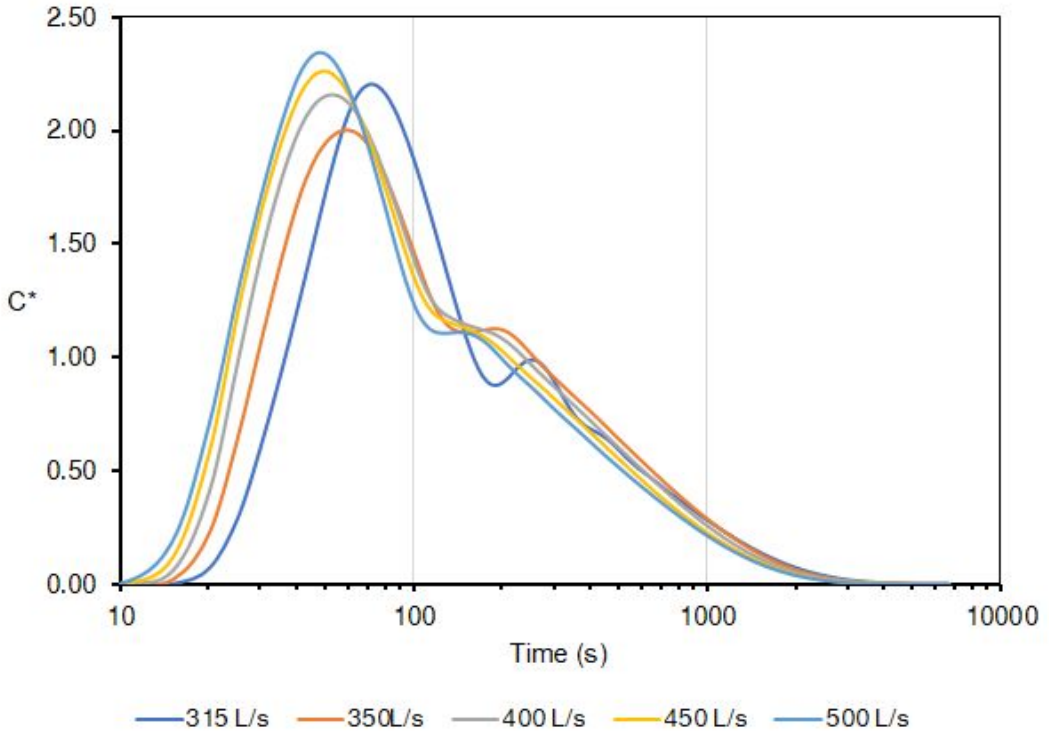

Figure 2.18: Normalized Average Concentration, C*, at the islands, for the cases with parallel FTI configuration.

Case	Q_{inlet} **(L/s)**	t_{mean1} **(s)**	t_{mean2} **(s)**	$\bar{t}_{mean}$ (s)
1	315	844	1173	1009
2	350	752	1131	942
3	400	740	997	869
4	450	618	950	784
5	500	634	860	747

Table 2.4: Estimated Mean Residence Time for each FTI in series

To understand if there is an influence of inlet tracer concentration over these results, the second series of simulations was run, and their results will be discussed in the next topic.

2.3.4 Different amounts of Mass entering the Pond

In the second step we first simulated a range of flow rates going from 315 L/s to 500 L/s with a tracer concentration of 0.01 g/L for all flow rates, which meant that

Case	Island conf.	Q_{inlet} (L/s)	$\bar{t}_{mean}$ (s)	%Muptake
1	Serial	315	1009	0.61
2	Serial	350	942	0.60
3	Serial	400	869	0.56
4	Serial	450	784	0.54
5	Serial	500	747	0.52
6	Parallel	315	692	0.59
7	Parallel	350	645	0.60
8	Parallel	400	597	0.56
9	Parallel	450	570	0.53
10	Parallel	500	550	0.50

Table 2.5: Estimated Mean Residence Time for each FTI system

different amounts of mass would be entering the pond. This was done only for the serial FTI configuration, as it was the one that showed the best overall performance. However, comparing the results of this series of simulations with those of the first one, there was no considerable difference, with the same fractional mass removal achieved for the first series of simulations being achieved by the corresponding flow rates of the latter.

For the case with Q = 500 L/s, which was the one with the greatest variation between mass injected in the first and the second steps, tracer mass injected was, respectively, 31.5 g and 50.0 g for each case. Its is interesting to highlight the fact that, even with a larger amount of tracer entering the pond for this case, it remained being the one with the worst removal performance, indicating that possibly the higher flow rate is leading to a less efficient hydrodynamics for treatment. To evaluate if the treatment for these cases is somehow dependent of the tracer amount injected, or if it only depends of the pond hydrodynamics, simulations with different tracer concentrations were run for Q = 315 L/s, first comparing it with the case of 500 L/s, injecting 50 g of tracer, then testing for higher values, injecting 2, 5 and 10 times the initial tracer amount for the original case. Table 2.6 presents the results from cases with same concentration. Case 1 is the same of the first series of simulations, because it already had the tested concentration of 0.01 g/L. The results show that the treatment performance achieved by the FTI system was not dependent of the amount of tracer injected in the pond. This means that the hydrodynamic conditions generated within the pond by each flow rate are the main factor leading to a better or worse performance. Cases with the same velocity field, only changing the mass injected, presented the same fractional removal. Other factors, however, can impact, and were not tested in this work. For all simulations, the tracer was inert and its mixture had the same density as water, conditions that may not occur for

actual treatment systems. Therefore, the effect of increasing tracer mass still needs to be tested simulating the injection of different pollutants, with different densities, to assess if there is any considerable difference, or if the hydrodynamics remains being the main aspect influencing over treatment.

Case	Q_{inlet} **(L/s)**	$M_{injected}$ **(g)**	$\%M_{uptake}$	$\%M_{FTI1}$	$\%M_{FTI2}$
1	315	31.5	0.61	0.42	0.33
11	350	35.0	0.60	0.41	0.32
12	400	40.0	0.56	0.34	0.33
13	450	45.0	0.54	0.35	0.29
14	500	50.0	0.52	0.32	0.29
15	315	50.0	0.61	0.42	0.33
16	315	63.0	0.61	0.42	0.33
17	315	157.5	0.61	0.42	0.33
18	315	315.0	0.61	0.42	0.33

Table 2.6: Mass uptake results for cases with different amounts of tracer entering the pond.

2.4 Conclusion

The mass removal performance of Floating Treatment Islands within stormwater ponds was investigated under a hydrodynamic perspective, through CFD simulations employing a Reynolds-Averaged Navier-Stokes (RANS) approach. Different inlet flow rates were tested, under a typical operating range of 300-500 L/s, for two different island positioning configurations: 2 islands in series and 2 islands in parallel. The velocity field was characterized and analyzed for each case, and the mass removal of the system and of each individual FTI was analyzed.

The overall system's tracer removal tended to decrease as the inlet flow rate (i.e. flow velocity) increased, and the serial islands configuration presented the best performance of both configurations. The flow deceleration and recirculation patterns were important factors for a better mass removal performance. Plus, the FTI configuration with the best performance was tested at the inlet flow rate that presented the best results, for different tracer amounts, in order to identify if the amount or concentration of tracer would have any interference over the results, and it was observed that the fractional removal remained the same for every scenario under the same flow conditions.

The results show that the mass removal by FTI is dependent of the flow conditions

that the system Pond+FTI generates. The best performances were recorded at the cases that presented reversed flow patterns leading to a higher mass of tracer entering the root zone of the islands, and those cases were the ones with an average velocity within the pond between 0.08 and 0.10 m/s. The retention time of the tracer inside the islands also shows to be an important factor, that still needs further research to a better understanding and modeling. To determine modeling and design guidelines for FTIs, it becomes clear that the island positioning must be determined on a way that favors flow deceleration and recirculation, ensuring longer residence times of the pollutants within the root zone, which will increase the mass uptake by the plants.

This study expanded the knowledge on how the hydrodynamics affects mass removal by Floating Treatment Islands, showing that the way flow occurs within a pond and across the root zone of the FTI is the key factor for its treatment performance. Understanding and modeling residence time within individual FTIs is also another relevant topic, that still needs to be more explored. These results may be useful for determining well founded design guidelines for FTIs and stormwater ponds, and its application in real-life macro-drainage systems.

References

ANSYS, Inc. ANSYS CFX Solver Theory Guide. In: [s.l.]: ANSYS, Inc., 2009. chap. 2. Cit. on p. 11.

BI, Ran et al. Giving waterbodies the treatment they need: A critical review of the application of constructed floating wetlands. **Journal of Environmental Management**, v. 238, p. 484–498, 2019. DOI: https://doi.org/10.1016/j.jenvman.2019.02.064. Available from: <https://www.sciencedirect.com/science/article/pii/S0301479719302154>. Cit. on pp. 2, 8.

BIRCH, G. F.; MATTHAI, C.; FAZELI, M. S. Efficiency of a retention/detention basin to remove contaminants from urban stormwater. **Urban Water Journal**, v. 3, n. 2, p. 69–77, 2006. DOI: https://doi.org/10.1080/15730620600855894. Cit. on p. 7.

CHEN, Zhengbing; JIANG, Chunbo; NEPF, Heidi. Flow adjustment at the leading edge of a submerged aquatic canopy. **Water Resources Research**, v. 49, n. 9, p. 5537–5551, 2013. DOI: https://doi.org/10.1002/wrcr.20403. eprint: https://agupubs.onlinelibrary.wiley.com/doi/pdf/10.1002/wrcr.20403. Available from: <https://agupubs.onlinelibrary.wiley.com/doi/abs/10.1002/wrcr.20403>. Cit. on p. 22.

CHUA, Lloyd H.C. et al. Treatment of baseflow from an urban catchment by a floating wetland system. **Ecological Engineering**, v. 49, p. 170–180, 2012. ISSN 0925-8574. DOI: https://doi.org/10.1016/j.ecoleng.2012.08.031. Available from: <https://www.sciencedirect.com/science/article/pii/S0925857412002911>. Cit. on pp. 8, 38.

GUALTIERI, Carlo et al. On the Values for the Turbulent Schmidt Number in Environmental Flows. **Fluids**, v. 2, n. 2, 2017. DOI: 10.3390/fluids2020017. Available from: <https://www.mdpi.com/2311-5521/2/2/17>. Cit. on p. 14.

GUZMÁN, Celina Balderas; COHEN, Samantha, et al. Island topographies to reduce short-circuiting in stormwater detention ponds and treatment wetlands. **Ecological Engineering**, v. 117, p. 182–193, 2018. DOI: https://doi.org/10.1016/j.ecoleng.2018.02.020. Available from: <https://www.sciencedirect.com/science/article/pii/S0925857418300582>. Cit. on pp. 4, 7, 37.

HEADLEY, Tom R.; TANNER, Chris C. Application of Floating Wetlands for Enhanced Stormwater Treatment: A Review. **NIWA Client Report**, v. 123, Jan. 2006. Available from: <https://www.researchgate.net/publication/266409739_Application_of_Floating_Wetlands_for_Enhanced_Stormwater_Treatment_A_Review>. Cit. on pp. 3, 4, 7.

_____. Constructed Wetlands With Floating Emergent Macrophytes: An Innovative Stormwater Treatment Technology. **Critical Reviews in Environmental Science and Technology**, Taylor Francis, v. 42, n. 21, p. 2261–2310, 2012. DOI: 10.1080/10643389.2011.574108. Available from: <https://doi.org/10.1080/10643389.2011.574108>. Cit. on pp. 4, 5, 7, 26.

KHAN, Sher. **Hydrodynamics of Sediment Retention Ponds**. 2012. PhD thesis – Dept. of Civil and Environmental Engineering, University of Auckland, Auckland, New Zealand. Cit. on pp. 4, 9, 15, 39.

KHAN, Sher; MELVILLE, Bruce W.; SHAMSELDIN, Asaad. Design of Storm-Water Retention Ponds with Floating Treatment Wetlands. **Journal of Environmental Engineering**, v. 139, n. 11, p. 1343–1349, 2013. DOI: 10.1061/(ASCE)EE.1943-7870.0000748. Available from: <https://ascelibrary.org/doi/10.1061/%28ASCE%29EE.1943-7870.0000748>. Cit. on pp. 4, 7, 8, 15, 24, 27, 38, 39.

KHAN, Sher; MELVILLE, Bruce W.; SHAMSELDIN, Asaad Y.; FISCHER, Christoph. Investigation of Flow Patterns in Storm Water Retention Ponds using CFD. **Journal of Environmental Engineering**, v. 139, n. 1, p. 61–69, 2013. DOI: 10.1061/(ASCE)EE.1943-7870.0000540. eprint:

https://ascelibrary.org/doi/pdf/10.1061/%28ASCE%29EE.1943-7870.0000540. Cit. on p. 8.

KHAN, Sher; SHOAIB, Muhammad, et al. Hydraulic investigation of the impact of retrofitting floating treatment wetlands in retention ponds. **Water Science and Technology**, v. 80, n. 8, p. 1476–1484, 2019. DOI: 10.2166/wst.2019.397. Available from: <https://doi.org/10.2166/wst.2019.397>. Cit. on pp. 4, 5, 8, 37–39, 45.

LADISLAS, S. et al. Performances of Two Macrophytes Species in Floating Treatment Wetlands for Cadmium, Nickel, and Zinc Removal from Urban Stormwater Runoff. **Water, Air, & Soil Pollution**, Springer Science and Business Media LLC, v. 224, n. 2, Jan. 2013. DOI: 10.1007/s11270-012-1408-x. Available from: <https://doi.org/10.1007/s11270-012-1408-x>. Cit. on pp. 8, 38.

MACHADO XAVIER, Manoel Lucas; JANZEN, Johannes Gerson; NEPF, Heidi. Numerical modeling study to compare the nutrient removal potential of different floating treatment island configurations in a stormwater pond. **Ecological Engineering**, v. 111, p. 78–84, 2018. DOI: https://doi.org/10.1016/j.ecoleng.2017.11.022. Available from: <https://www.sciencedirect.com/science/article/pii/S092585741730633X>. Cit. on pp. 4, 5, 8–10, 15, 17, 18, 21–26, 38, 39, 41, 42.

MENTER, F. R.; KUNTZ, M.; LANGTRY, R. Ten Years of Industrial Experience with the SST Turbulence Model. **Turbulence, Heat and Mass Transfer 4**, v. 1, p. 625–632, 2003. DOI: 10.1.1.460.2814. Cit. on pp. 12, 14, 41.

PAVLINERI, Natalia; SKOULIKIDIS, Nikolaos Th.; TSIHRINTZIS, Vassilios A. Constructed Floating Wetlands: A review of research, design, operation and management aspects, and data meta-analysis. **Chemical Engineering Journal**, v. 308, p. 1120–1132, 2017. DOI: https://doi.org/10.1016/j.cej.2016.09.140. Available from: <https://www.sciencedirect.com/science/article/pii/S1385894716313857>. Cit. on pp. 2, 3, 8, 38.

PERSSON, J. The hydraulic performance of ponds of various layouts. **Urban Water**, v. 2, n. 3, p. 243–250, 2000. DOI: https://doi.org/10.1016/S1462-0758(00)00059-5. Available from: <https://www.sciencedirect.com/science/article/pii/S1462075800000595>. Cit. on pp. 4, 7.

ROMINGER, JEFFREY T.; NEPF, HEIDI M. Flow adjustment and interior flow associated with a rectangular porous obstruction. **Journal of Fluid Mechanics**, Cambridge University Press (CUP), v. 680, p. 636–659, June 2011. DOI: 10.1017/jfm.2011.199. Available from: <https://doi.org/10.1017/jfm.2011.199>. Cit. on p. 23.

SABOKROUHIYEH, Nima et al. A numerical study of the effect of wetland shape and inlet-outlet configuration on wetland performance. **Ecological Engineering**, v. 105, p. 170–179, 2017. ISSN 0925-8574. DOI: https://doi.org/10.1016/j.ecoleng.2017.04.062. Available from: <https://www.sciencedirect.com/science/article/pii/S0925857417302471>. Cit. on p. 21.

VYMAZAL, Jan. Removal of nutrients in various types of constructed wetlands. **Science of The Total Environment**, v. 380, n. 1, p. 48–65, 2007. DOI: https://doi.org/10.1016/j.scitotenv.2006.09.014. Available from: <https://www.sciencedirect.com/science/article/pii/S0048969706007212>. Cit. on pp. 2, 8.

Chapter 3

How Root Depths Impact Mass Removal by Floating Treatment Islands

In this chapter, the second specific objective of the dissertation is presented. The goal of this topic was to describe the influence of root depths from floating treatment islands within stormwater ponds, in order to get a better understanding of the behavior of those systems.

3.1 Introduction

Floating Treatment Islands (FTI) are an innovative solution for water treatment in lakes, ponds, reservoirs and also rivers, being an alternative to conventional subsurface-flow constructed wetlands. One of their main advantages over the conventional wetland systems is that their roots, since are not in the soil, are forced to absorb nutrients from the water, which is helpful for the removal of pollutants or substances present in excessive quantities in the water, such as Phosphorus, Nitrogen, Copper, Zinc and Suspended Solids (KADLEC; WALLACE, 2008; TANNER; HEADLEY, 2011).

Studies have shown that the presence of a FTI within a stormwater pond can significantly improve its hydraulic performance, which also means improving its pollutant retention capability (KHAN; SHOAIB, et al., 2019). Another benefit of the use of FTI is their role for ecosystem services and habitat biodiversity on the sites they're located (NAKAMURA; MUELLER, 2008; GUZMÁN; COHEN, et al., 2018). Therefore, studies on their behavior, viability and determination of guidelines for their efficient application

are relevant for making possible to implement this solution on a larger scale.

In conventional subsurface wetland systems, the proper operating conditions require a relatively shallow water depth to be effective, due to the vegetation standing under water, meaning that higher depths or an increase on turbidity could affect negatively the system's performance (WU et al., 2015). On the other hand, Floating Treatment Islands are not affected by those factors, since the plants are above the water level, with only their roots submerged. This also means that the root mat under the FTI can be deeper than the height of conventional wetlands plants. This makes possible even the use of artificial roots containing biofilm to perform nutrient uptake, despite this solution does not offer a performance as effective as with natural roots (TANNER; HEADLEY, 2011).

Most of the published works on FTI applications are mesocosm studies, as shown in Pavlineri, Skoulikidis, and Tsihrintzis (2017), or investigations focused on water quality or biochemical aspects (CHUA et al., 2012; LADISLAS et al., 2013; WINSTON et al., 2013; KEIZER-VLEK et al., 2014; LU; KU; CHANG, 2015; TROITSKY et al., 2019). Recent works such as Khan, Melville, and Shamseldin (2013) and Khan, Shoaib, et al. (2019) provided a different approach for analyzing FTI, this time focusing on their impact over stormwater pond hydraulic performance. Finally, Machado Xavier, Janzen, and Nepf (2018) presented another approach, still focusing on hydrodynamics, but this time analyzing the impact of FTI configuration and positioning within the pond over nutrient removal by the islands, which gave new possibilities to evaluate and design FTI to ensure good water treatment, not only by the pond, but also by each individual island. This work keeps on the same approach.

The hydrodynamic behavior of root systems with different depths have been studied by (KHAN; SHOAIB, et al., 2019), concluding that an optimal relative depth of the roots is of 0.50, to achieve the best pond performance. However, the removal potential of the FTI with different root depths was not analyzed. Evaluating it would help to design FTI structures optimizing the pond hydraulics and nutrient removal, besides helping to understand how the plant and root growth might interfere over the velocity field within the pond.

The objective of this study was to understand how the depth of roots affect on mass removal by FTIs, individually and as a system. Khan, Shoaib, et al. (2019) analyzed the influence that roots have over the pond's hydraulic performance, but not how this interferes over the nutrient removal by the FTIs, and this is the goal of the present paper. To accomplish the objectives, numerical simulations were undertaken using Computational Fluid Dynamics (CFD) techniques, based on a real scale version of the model used by Machado Xavier, Janzen, and Nepf (2018).

3.2 Methods

To achieve the objetives of the study, numerical simulations were undertaken, using a student's license of the commercial software ANSYS Workbench - 2020 R2. Geometry was designed using the software ANSYS Design Modeler, spatial discretization employed ANSYS Meshing, and the simulation itself, setting boundary conditions and running the calculation by a Finite-Volume Method (FVM), was done using the ANSYS CFX. Post-processing of the results employed ANSYS CFD Post. The steps mentioned above will be briefly described in this topic.

3.2.1 Geometry and Spatial Discretization

The geometry was a full-scale model of that described at Khan (2012), Khan, Melville, and Shamseldin (2013) and Khan, Shoaib, et al. (2019), and consisted of a 41 m long, 15 m wide and 2.3 m deep stormwater pond, with sloping walls at 0.50 m/m slope each side. The flow inlet was a circular pipe with diameter of 450 mm, and the outlet pipe had a diameter of 1.05 m. The FTI system consisted of two islands positioned in parallel, with plan dimensions of 6.0 m long and 7.7 m wide. The root zone height (L_R) of the FTI varied from 0.58 m to 1.63 m for each case, which represents a range of relative root depths (L_R/D_P, where D_P is the pond depth) between 0.25 and 0.71. A scheme of the pond Geometry is shown at Figure 3.1.

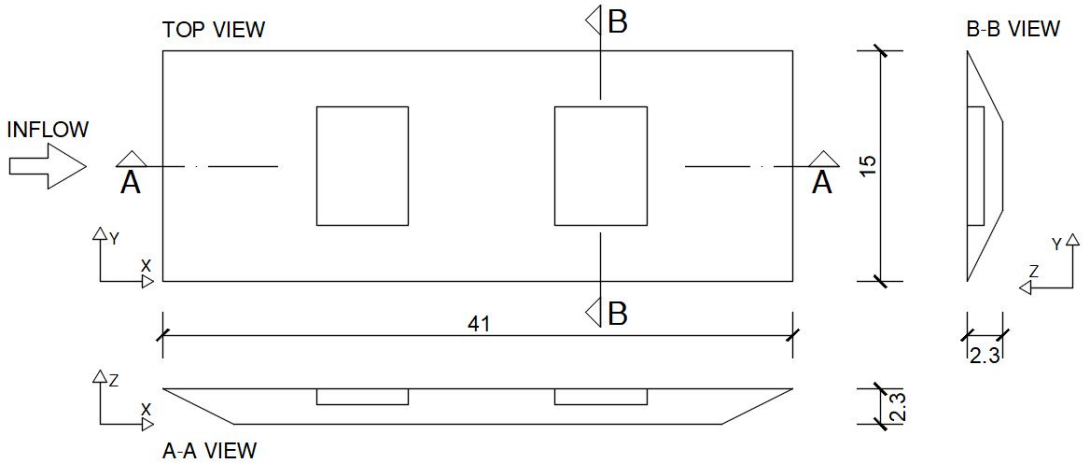

Figure 3.1: Scheme of the pond geometry. Units in meters.

Six cases were run, each one with a different root depth. The cases were named from R1 to R6, with the highest index meaning the longest root depth. Model validation was not necessary, because it was already validated by Machado Xavier, Janzen, and Nepf (2018), where details about this step can be found. The case R3 is a 1:1 scale of Case 1 of the mentioned work, and presented the same mass removal results, thus con-

firming the scale similarity between the models. Details on the root geometry for each case are shown on Table 3.1. The fraction of pond volume is relative to the pair of FTIs. The root depths were set based on their relative length to the maximum depth of the pond.

Case	L_R **(m)**	L_R/D_P	**Root zone volume (m³)**	**Fraction of Pond Volume**
R1	0.58	0.25	26.57	0.06
R2	0.80	0.35	36.96	0.08
R3	1.05	0.46	48.51	0.11
R4	1.15	0.50	53.13	0.12
R5	1.50	0.65	69.30	0.16
R6	1.63	0.71	75.31	0.17

Table 3.1: Root zone geometry details for each case.

The meshing procedure for the spatial discretization was done using the ANSYS Meshing software, generating an unstructured mesh for each geometry. To ensure a highly accurate response on the results, the most important regions for the development of the velocity field and for analyzing flow through the FTIs were treated with finer numerical grids. Inflow and outflow exit regions, the root zones and regions with flow closer to the islands were the main zones of interest on refining the mesh. For each of the 6 cases tested in this work, the number of elements was in the order of 10^5 elements, which falls into the maximum number of elements allowed by the academic version of ANSYS Workbench. Details on the numerical grid are shown in Figure 3.2.

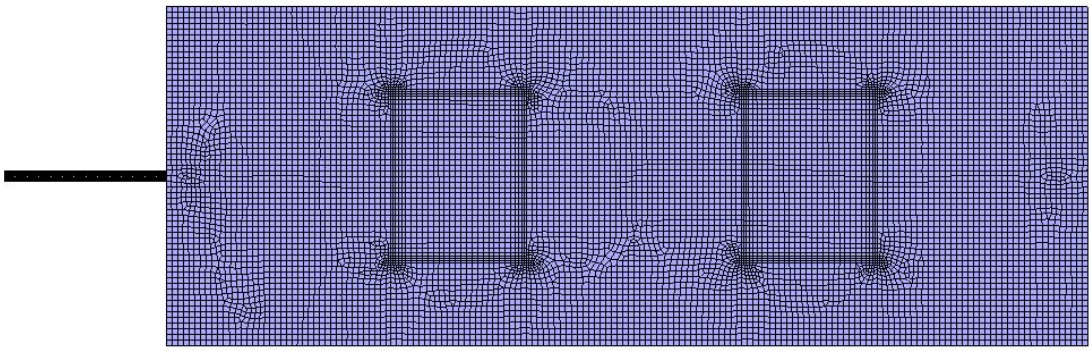

Figure 3.2: Top view of a part of the mesh. The regions with highest sensibility to the discretization present a finer grid.

3.2.2 Flow Modeling and Boundary Conditions

Flow within the pond was modelled and simulated with the aid of numerical code ANSYS CFX 2020 R2. The transport equations were modelled using a Reynolds-Averaged

Navier-Stokes (RANS) formulation. The Reynolds-averaged equations for continuity and momentum are shown below:

$$\frac{\partial \rho}{\partial t} + \frac{\partial}{\partial x_i}\big(\rho U_i\big) = 0 \tag{3.1}$$

$$\frac{\partial \rho U_i}{\partial t} + \frac{\partial}{\partial x_j}\big(\rho U_i U_j\big) = -\frac{\partial p}{\partial x_i} + \frac{\partial}{\partial x_j}\big(\tau_{ij} - \rho\overline{u_i u_j}\big) + S_{M,i} \tag{3.2}$$

With ρ being the fluid density, i,j = 1, 2 or 3, respectively; U, the velocity vector; τ_{ij}, the molecular stress tensor; $\overline{u_i u_j}$, the Reynold stress, where u_i is the time varying component of velocity, due to turbulent fluctuations; and $S_{M,i}$, the momentum source, that represented, in this case, the root zone drag.

Turbulence is a key factor to represent FTI's mass removal within stormwater ponds, and for this work the chosen model was the Shear-Stress Transport (SST) k-omega model (MENTER; KUNTZ; LANGTRY, 2003), due to its capability of providing well accurate results for turbulence flow modeling at free stream and also near-wall boundary layer regions, with a relatively low computational effort when compared to stronger turbulence models. The transient scheme chosen for the cases was a Second Order Backward Euler. As boundary conditions, an uniform flow at the inlet was set, with constant velocity of 2 m/s, meaning a flow rate of 315 L/s entering the pond. At the outlet, a gauge pressure of 0 Pa was specified. The walls had no-slip boundary conditions and the free-surface was considered a symmetry plane with zero gradient normal to it.

To represent the FTI's root zone, we employed a porous-media approach, due to its relative simplicity and lower computational effort than if a complex root geometry was chosen. The porous media effect on the flow was represented using the momentum source

$$S_{M,i} = \frac{\mu}{K_{perm}} U_i \tag{3.3}$$

With K_{perm} being the permeability of the root zone. The value of permeability was set as K_{perm}=10^{-6} m^2, which was based on a series of tests with different coefficients, being the one with the best results for the velocity field and treatment performance.

Concentration within the pond was calculated using conservation of mass, setting a value of 1 for the turbulent Schmidt number (Sc=ν_t/D_t) (MACHADO XAVIER; JANZEN; NEPF, 2018), at the following equation:

$$\frac{\partial C}{\partial t} + \frac{\partial (u_i C)}{\partial x_i} = \frac{\partial}{\partial x_i}\left(\frac{v_t}{Sc}\frac{\partial C}{\partial x_i}\right) - k_r C \tag{3.4}$$

Where ν_t is the kinematic viscosity, D_t is the turbulent diffusivity, and k_r is the first-order rate constant, which was used to describe mass removal within the root zones as a first-order decay reaction. In this study, k_r was set as 0.0071, only at root zones, which makes the normalized values of $k_r tn$ of all cases fall within the range described by Machado Xavier, Janzen, and Nepf (2018). For the rest of the domain, k_r was set to zero.

After all these conditions were set, the simulation procedure was the following: First, the velocity field of each case was determined running permanent flow regime simulations. Then, tracer studies were simulated for each root depth, divided into two transient simulations each: in the first, the decay reaction representing mass removal by the roots was turned off, and tracer was injected at a concentration of 0.01 g/L, simulated as a 10 s pulse, meaning that for each case, 31.5 g of tracer were injected. This first simulation was run until 95% of the tracer mass had exited the pond. Then, with the decay reaction enabled at the root zones, another simulation was run for the same time.

3.2.3 Post-processing and Measured Parameters

Results were analyzed and post-processed using ANSYS CFD Post. Velocity vectors and contours for each case were generated to provide a qualitative analysis of the flow fields within the pond under each root depth. To determine the amounts of mass leaving the pond at each step of the simulated cases, tracer concentration was measured at the pond outlet. The tracer mass exiting the pond, M_e was calculated by integrating the exit concentration, $C_{out}(t)$, multiplied by the flow rate:

$$M_e = \int_0^t Q C_{out}(t)\, dt \tag{3.5}$$

The fractional mass removal, $\%M_{uptake}$ of the system was defined as being 1 minus the ratio of mass exiting the pond (M_e) to the mass injected at the pond (M), as shown in the equation below:

$$\%M_{uptake} = 1 - \frac{M_e}{M} \tag{3.6}$$

To assess the contribution of each individual FTI of the system for mass removal at the pond, extra simulations were run enabling the decay reaction term for only one

FTI at a time. This way, assessing the mass passing the cross-section directly upstream of the FTI, M_{in}, and the mass passing the cross-section directly downstream the FTI, M_{out}, we were able to determine the fraction of tracer reaching the cross-section of each island, and thus evaluate the performance of each. The contribution of an individual FTI, $\%M_{FTI}$ was calculated by the expression:

$$\%M_{FTI} = \frac{(M_{in} - M_{out})}{M_{in}} \tag{3.7}$$

3.3 Results and Discussion

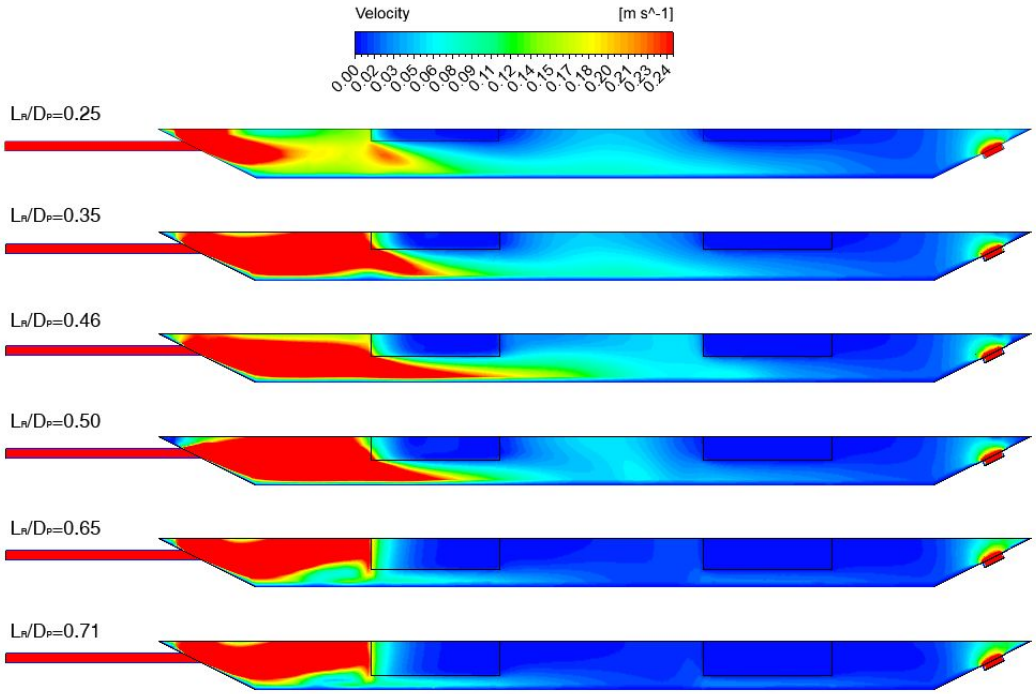

Figure 3.3: Velocity contours of each case, with different root depths.

The velocity fields within the pond presented great variation among the tested cases. As can be seen in Figure 3.3, there are basically three different scenarios occuring, depending on the root depth. The case with L_R/D_P=0.25 showed that the root zone is not reaching a depth enough for creating a great acceleration zone towards the bottom of the pond, which made the flow present a sharper deceleration, which may have led to more mixing and less tracer entering the root zone. This can explain, together with the smaller contact area of shorter roots to uptake the tracer, the worst mass removal results by this FTI's root configuration, as shown in Figure 3.4, whose results are summarized in Table 3.2. For cases R2, R3 and R4, the flow pattern have shown a deceleration plus recirculation near the leading edge of the upstream FTI. The first island caused a deceleration at the top regions of the pond, and an acceleration zone below the island, at

the bottom region of the pond. Mass uptake by the roots, in those cases, appears to be influenced by the recirculation leading tracer to the FTI root zone.

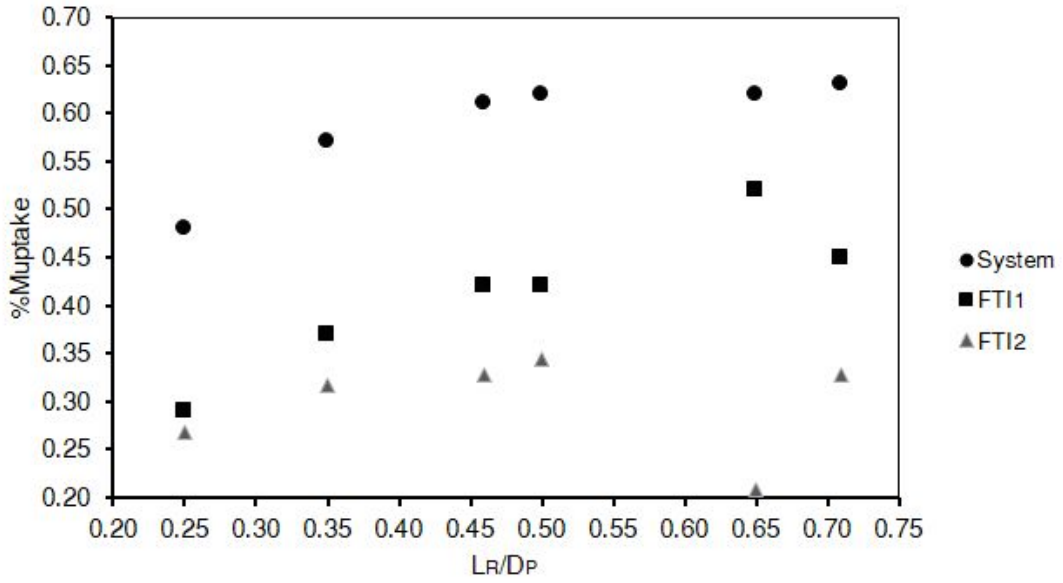

Figure 3.4: Mass Uptake vs Relative Root Depth for the system and for each individual FTI.

In the cases of L_R/D_P=0.65 and 0.71, flow blockage by the upstream FTI was such that the velocities at the bottom of the pond were much lower than in the other cases. Figure 3.5 shows the streamwise velocity at the upstream FTI, normalized by the streamwise velocity at the FTI leading edge, for all cases. Cases R5 and R6 present a different pattern of average streamwise velocity. While in the other cases, after x/h = 1.5, recirculation within the root zone tends to be preponderant, for R5 and R6, the streamwise velocity profile shows no negative values alongside the length of the upstream FTI. This indicates that the higher mass uptake by the higher values of L_R/D_P are most probably due to the higher area of the root zone in contact with the inflow jet, which allows a greater amount of tracer to be captured by the roots.

Case	L_R **(m)**	L_R/D_P	$\%M_{uptake}$	$\%M_{FTI1}$	$\%M_{FTI2}$
R1	0.58	0.25	0.48	0.29	0.27
R2	0.80	0.35	0.57	0.37	0.32
R3	1.05	0.46	0.61	0.42	0.33
R4	1.15	0.50	0.62	0.42	0.34
R5	1.50	0.65	0.62	0.52	0.21
R6	1.63	0.71	0.63	0.45	0.33

Table 3.2: Values of mass uptake by each case.

It is possible to see that the removal obtained by the islands tends to increase

with the deeper root zones. However, this increase is not much significant for those cases with roots longer than half the pond depth (L_R/D_P>0.50). Khan, Shoaib, et al. (2019) assessed by his experimenters that, under a hydraulic pond performance point of view, analyzing the occurrence of short circuiting and mixing within the pond, the optimal relative root depth was 0.50, and our results also show that from 0.45 to 0.50, the mass removal performance shows good results without having to appeal to much deeper roots, which are also more difficult to find and use. The need of roots excessively deep could lead to the necessity of employing artificial root mats with biofilm, which would be expensive and not as effective as natural roots, as shown by Tanner and Headley (2011). Analyzing individual FTI performance, the tendency was of an increasing mass uptake by the upstream islands, while the downstream FTI did not appear to be much affected by the depth of the roots, except for the case R5, which presented the lower values of $\%M_{uptake}$. The flow pattern generated by the upstream island makes that the tracer availability to enter the root zone of the downstream FTI be so low that the performance is almost not affected by any change in its geometry. The normalized streamwise velocity at the downstream FTI have shown similar patterns among all tested cases, as shown in Figure 3.6.

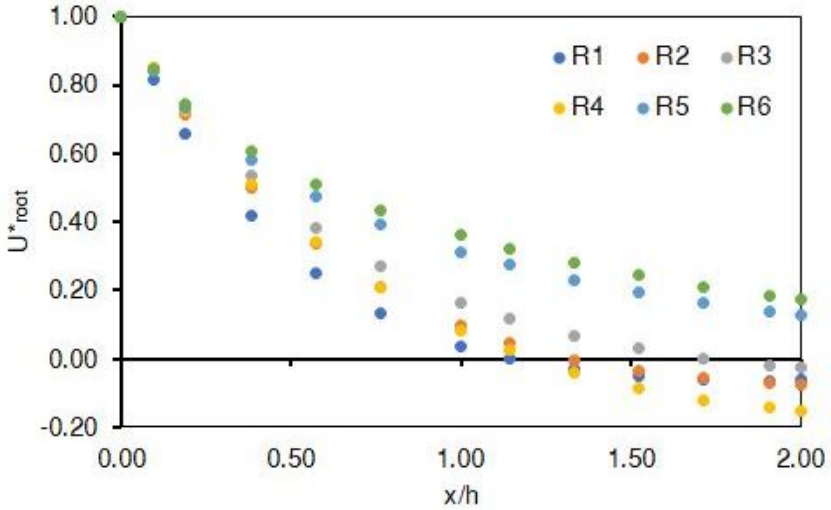

Figure 3.5: Comparison of the normalized streamwise velocities, $U*_{root}$, at the upstream FTI.

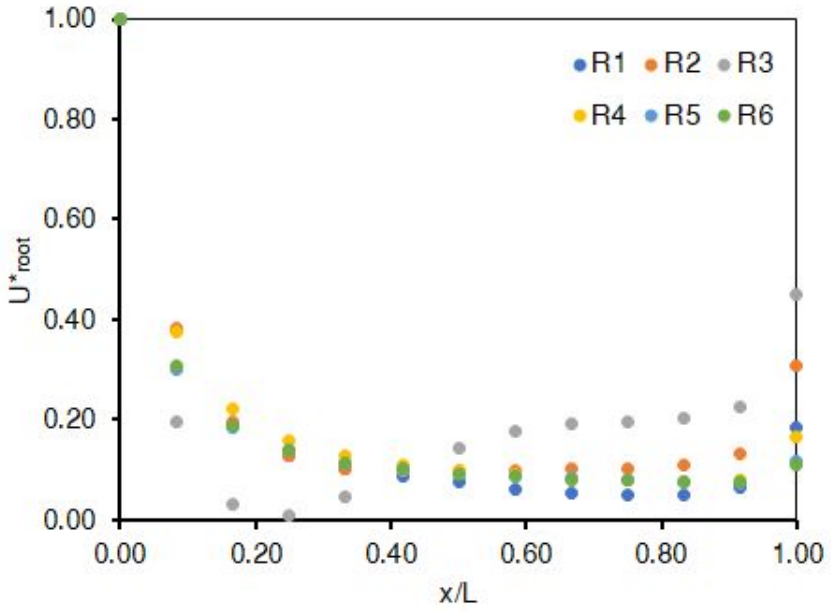

Figure 3.6: Comparison of the normalized streamwise velocities, $U*_{root}$, at the downstream FTI.

3.4 Conclusion

Tracer studies in a full-scale stormwater pond containing Floating Treatment Islands with different root depths were simulated, using the academic version of a numerical Finite-Volume Method commercial code. Results indicate that cases with deeper roots present the greater nutrient removal potential. However, the performance gain due to the increase in the depth of roots have shown to be little after a certain point, for relative root depths, L_R/D_P, above 0.46. This indicates that an optimal value for the root depth within a stormwater pond, under a hydrodynamic perspective of the treatment processes, is about half the depth of the pond. Also, the length of the roots presents great influence over the velocity field within the pond, which appears to be essential for a more efficient mass uptake performance by the root zones of the FTI.

References

CHUA, Lloyd H.C. et al. Treatment of baseflow from an urban catchment by a floating wetland system. **Ecological Engineering**, v. 49, p. 170–180, 2012. ISSN 0925-8574. DOI: https://doi.org/10.1016/j.ecoleng.2012.08.031. Available from: <https://www.sciencedirect.com/science/article/pii/S0925857412002911>. Cit. on pp. 8, 38.

GUZMÁN, Celina Balderas; COHEN, Samantha, et al. Island topographies to reduce short-circuiting in stormwater detention ponds and treatment wetlands. **Ecological Engineering**, v. 117, p. 182–193, 2018. DOI: https://doi.org/10.1016/j.ecoleng.2018.02.020. Available from: <https://www.sciencedirect.com/science/article/pii/S0925857418300582>. Cit. on pp. 4, 7, 37.

KADLEC, Robert H.; WALLACE, Scott. **Treatment Wetlands**. [S.l.]: CRC Press, July 2008. DOI: 10.1201/9781420012514. Available from: <https://doi.org/10.1201/9781420012514>. Cit. on p. 37.

KEIZER-VLEK, Hanneke E. et al. The contribution of plant uptake to nutrient removal by floating treatment wetlands. **Ecological Engineering**, Elsevier BV, v. 73, p. 684–690, Dec. 2014. DOI: 10.1016/j.ecoleng.2014.09.081. Available from: <https://doi.org/10.1016/j.ecoleng.2014.09.081>. Cit. on p. 38.

KHAN, Sher. **Hydrodynamics of Sediment Retention Ponds**. 2012. PhD thesis – Dept. of Civil and Environmental Engineering, University of Auckland, Auckland, New Zealand. Cit. on pp. 4, 9, 15, 39.

KHAN, Sher; MELVILLE, Bruce W.; SHAMSELDIN, Asaad. Design of Storm-Water Retention Ponds with Floating Treatment Wetlands. **Journal of Environmental Engineering**, v. 139, n. 11, p. 1343–1349, 2013. DOI: 10.1061/(ASCE)EE.1943-7870.0000748. Available from: <https://ascelibrary.org/doi/10.1061/%28ASCE%29EE.1943-7870.0000748>. Cit. on pp. 4, 7, 8, 15, 24, 27, 38, 39.

KHAN, Sher; SHOAIB, Muhammad, et al. Hydraulic investigation of the impact of retrofitting floating treatment wetlands in retention ponds. **Water Science and Technology**, v. 80, n. 8, p. 1476–1484, 2019. DOI: 10.2166/wst.2019.397. Available from: <https://doi.org/10.2166/wst.2019.397>. Cit. on pp. 4, 5, 8, 37–39, 45.

LADISLAS, S. et al. Performances of Two Macrophytes Species in Floating Treatment Wetlands for Cadmium, Nickel, and Zinc Removal from Urban Stormwater Runoff. **Water, Air, & Soil Pollution**, Springer Science and Business Media LLC, v. 224, n. 2, Jan. 2013. DOI: 10.1007/s11270-012-1408-x. Available from: <https://doi.org/10.1007/s11270-012-1408-x>. Cit. on pp. 8, 38.

LU, Hsiao-Ling; KU, Chen-Ruei; CHANG, Yuan-Hsiou. Water quality improvement with artificial floating islands. **Ecological Engineering**, Elsevier BV, v. 74, p. 371–375, Jan. 2015. DOI: 10.1016/j.ecoleng.2014.11.013. Available from: <https://doi.org/10.1016/j.ecoleng.2014.11.013>. Cit. on p. 38.

MACHADO XAVIER, Manoel Lucas; JANZEN, Johannes Gerson; NEPF, Heidi. Numerical modeling study to compare the nutrient removal potential of different floating treatment island configurations in a stormwater pond. **Ecological Engineering**, v. 111, p. 78–84, 2018. DOI: https://doi.org/10.1016/j.ecoleng.2017.11.022. Available from: <https://www.sciencedirect.com/science/article/pii/S092585741730633X>. Cit. on pp. 4, 5, 8–10, 15, 17, 18, 21–26, 38, 39, 41, 42.

MENTER, F. R.; KUNTZ, M.; LANGTRY, R. Ten Years of Industrial Experience with the SST Turbulence Model. **Turbulence, Heat and Mass Transfer 4**, v. 1, p. 625–632, 2003. DOI: 10.1.1.460.2814. Cit. on pp. 12, 14, 41.

NAKAMURA, K.; MUELLER, G. Review of the Performance of the Artificial Floating Island as a Restoration Tool for Aquatic Environments. In: WORLD ENVIRONMENTAL AND WATER RESOURCES CONGRESS 2008, Ahupua'a. American Society of Civil Engineers. DOI: 10.1061/40976(316)276. Available from: <https://ascelibrary.org/doi/10.1061/40976%28316%29276>. Cit. on pp. 4, 37.

PAVLINERI, Natalia; SKOULIKIDIS, Nikolaos Th.; TSIHRINTZIS, Vassilios A. Constructed Floating Wetlands: A review of research, design, operation and management aspects, and data meta-analysis. **Chemical Engineering Journal**, v. 308, p. 1120–1132, 2017. DOI: https://doi.org/10.1016/j.cej.2016.09.140. Available from: <https://www.sciencedirect.com/science/article/pii/S1385894716313857>. Cit. on pp. 2, 3, 8, 38.

TANNER, Chris C.; HEADLEY, Tom R. Components of floating emergent macrophyte treatment wetlands influencing removal of stormwater pollutants. **Ecological Engineering**, Elsevier BV, v. 37, n. 3, p. 474–486, Mar. 2011. DOI: 10.1016/j.ecoleng.2010.12.012. Available from: <https://doi.org/10.1016/j.ecoleng.2010.12.012>. Cit. on pp. 37, 38, 45.

TROITSKY, Brendan et al. Nutrient processes and modeling in urban stormwater ponds and constructed wetlands. **Canadian Water Resources Journal / Revue canadienne des ressources hydriques**, Informa UK Limited, v. 44, n. 3, p. 230–247, Apr. 2019. DOI: 10.1080/07011784.2019.1594390. Available from: <https://doi.org/10.1080/07011784.2019.1594390>. Cit. on p. 38.

WINSTON, Ryan J. et al. Evaluation of floating treatment wetlands as retrofits to existing stormwater retention ponds. **Ecological Engineering**, Elsevier BV, v. 54, p. 254–265, May 2013. DOI: 10.1016/j.ecoleng.2013.01.023. Available from: <https://doi.org/10.1016/j.ecoleng.2013.01.023>. Cit. on p. 38.

WU, Haiming et al. A review on the sustainability of constructed wetlands for wastewater treatment: Design and operation. **Bioresource Technology**, Elsevier BV,

v. 175, p. 594–601, Jan. 2015. DOI: 10.1016/j.biortech.2014.10.068. Available from: <https://doi.org/10.1016/j.biortech.2014.10.068>. Cit. on p. 38.

Chapter 4

Conclusion and Recommendations

The objective of this dissertation, was to analyze how the hydrodynamics of the flow within stormwater ponds containing Floating Treatment Islands impacted over the mass removal by these systems. Numerical studies were undertaken to achieve this goal, evaluating the effects of flow rates entering the pond and of the depth of FTI's root zones.

In the first chapter, a brief literature review was done, to show and explain the scientific background and gaps to be explored, that served as motivation for this study. The second chapter presented a numerical study, to describe and evaluate the flow conditions occurring within a stormwater pond with FTIs of same relative volume, at two different island positioning arrangements (serial and parallel) and under 5 different flow rates entering the pond, all of them within the usual operational range found in the literature. The system Pond+FTI have shown to be dependent of the flow conditions, especially the deceleration and recirculation patterns, which affected considerably the mass uptake by the system and, especially, by the FTI directly in contact with the inflow jet. Under a qualitative evaluation, the cases with the best performance were those that presented recirculation zones directly leading to the FTI root zones. The serial configuration shown a better overall performance than the parallel, but the results of both configurations were close, in the order of 0.01. The cases with the best performance were those with an average velocity within the pond between 0.08 and 0.10 m/s, favoring both reversed flow and residence time at the root zones. Each configuration catches the pollutants entering the pond in a different way, with the inflow jet entering the upstream FTI of the serial cases directly at the leading edge, while in the parallel cases, a significant portion of flow enters by the inner sides' faces of the FTIs. Another important result was that the fractional mass uptake by the roots is not dependent of the amount of tracer entering the pond, but only of the flow conditions generated within the pond. The third chapter presented a numerical study on the influence of root depths within the pond. Root zones

covering higher fractions of the pond depth have shown better mass removal performance. However, their performance was not much better than the cases with roots about half of the depth of the pond, showing that an optimal relative root depth is of approximately half the pond depth, between 0.45 and 0.50, which can also helpful for economical and technical viability reasons.

This dissertation helped to expand the existing knowledge about Floating Treatment Islands, showing that the impact of the combined factors of FTI configuration (island positioning and root depths) and the velocity fields generated under operational conditions have great relevance for the mass removal performance of the system. This study showed that the removal performance of an FTI system is related to the velocity field characteristics. The systems with the best performance are those whose velocity fields and recirculation characteristics lead to a higher fraction of pollutant mass entering the FTI root zones. When the FTI is positioned at a region with a velocity field without relevant recirculation, tracer availability presents little variation, and remains low. Future studies evaluating the flow velocity reduction by testing different inflow pipe diameters are indicated to assess their influence, for regions presenting higher typical rainfall runoff. The root zone characteristics have also shown to be another factor interfering over the flow conditions within a stormwater ponds. Their influence over situations of flooding and varying water levels at the pond still need to be analyzed in future research. The contributions of this work are expected to be useful for the determination of standard design guidelines for Floating Treatment Islands, aiming for its optimization under a hydrodynamic perspective of the nutrient removal achieved by these systems.

References

ANSYS, Inc. ANSYS CFX Solver Theory Guide. In: [s.l.]: ANSYS, Inc., 2009. chap. 2. Cit. on p. 11.

BI, Ran et al. Giving waterbodies the treatment they need: A critical review of the application of constructed floating wetlands. **Journal of Environmental Management**, v. 238, p. 484–498, 2019. DOI: https://doi.org/10.1016/j.jenvman.2019.02.064. Available from: <https://www.sciencedirect.com/science/article/pii/S0301479719302154>. Cit. on pp. 2, 8.

BIRCH, G. F.; MATTHAI, C.; FAZELI, M. S. Efficiency of a retention/detention basin to remove contaminants from urban stormwater. **Urban Water Journal**, v. 3, n. 2, p. 69–77, 2006. DOI: https://doi.org/10.1080/15730620600855894. Cit. on p. 7.

BRIX, Hans. Use of constructed wetlands in water pollution control: historical development, present status, and future perspectives. **Water Science and Technology**, v. 30, n. 8, p. 209–223, 1994. DOI: 10.2166/wst.1994.0413. Available from: <https://iwaponline.com/wst/article/30/8/209/27999/Use-of-constructed-wetlands-in-water-pollution>. Cit. on p. 1.

CHARACKLIS, Gregory W.; WIESNER, Mark R. Entry and Deposits of Suspended Particulate Matter in Groyne Fields of the Middle Elbe and its Ecological Relevance. **Journal of Environmental Engineering**, v. 123, n. 8, p. 753–759, 1997. DOI: 10.1061/(ASCE)0733-9372(1997)123:8(753). Available from: <https://doi.org/10.1061/(ASCE)0733-9372(1997)123:8(753)>. Cit. on p. 1.

CHEN, Zhengbing; JIANG, Chunbo; NEPF, Heidi. Flow adjustment at the leading edge of a submerged aquatic canopy. **Water Resources Research**, v. 49, n. 9, p. 5537–5551, 2013. DOI: https://doi.org/10.1002/wrcr.20403. eprint: https://agupubs.onlinelibrary.wiley.com/doi/pdf/10.1002/wrcr.20403. Available from: <https://agupubs.onlinelibrary.wiley.com/doi/abs/10.1002/wrcr.20403>. Cit. on p. 22.

CHEN, Zhongbing; CUERVO, Diego Paredes, et al. Hydroponic root mats for wastewater treatment—a review. **Environmental Science and Pollution Research**,

v. 23, p. 15911–15928, 2016. DOI: 10.1007/s11356-016-6801-3. Available from: <https://link.springer.com/article/10.1007/s11356-016-6801-3>. Cit. on pp. 3, 5.

CHUA, Lloyd H.C. et al. Treatment of baseflow from an urban catchment by a floating wetland system. **Ecological Engineering**, v. 49, p. 170–180, 2012. ISSN 0925-8574. DOI: https://doi.org/10.1016/j.ecoleng.2012.08.031. Available from: <https://www.sciencedirect.com/science/article/pii/S0925857412002911>. Cit. on pp. 8, 38.

ENI, Devalsam I. et al. Impact of urbanization on sub-surface water quality in Calabar Municipality, Nigeria. **International Journal of Humanities and Social Science**, v. 1, n. 10, p. 167–172, 2011. ISSN 2221-0989. Available from: <http://www.ijhssnet.com/journals/Vol_1_No_10_August_2011/21.pdf>. Cit. on p. 1.

GUALTIERI, Carlo et al. On the Values for the Turbulent Schmidt Number in Environmental Flows. **Fluids**, v. 2, n. 2, 2017. DOI: 10.3390/fluids2020017. Available from: <https://www.mdpi.com/2311-5521/2/2/17>. Cit. on p. 14.

GUZMÁN, Celina Balderas; COHEN, Samantha, et al. Island topographies to reduce short-circuiting in stormwater detention ponds and treatment wetlands. **Ecological Engineering**, v. 117, p. 182–193, 2018. DOI: https://doi.org/10.1016/j.ecoleng.2018.02.020. Available from: <https://www.sciencedirect.com/science/article/pii/S0925857418300582>. Cit. on pp. 4, 7, 37.

GUZMÁN, Celina Balderas; NEPF, Heidi; BERGER, Alan M. **Design Guidelines for Urban Stormwater Wetlands**. [S.l.], 2018. Available from: <https://dusp.mit.edu/publication/design-guidelines-urban-stormwater-wetlands>. Cit. on p. 1.

HEADLEY, Tom R.; TANNER, Chris C. Application of Floating Wetlands for Enhanced Stormwater Treatment: A Review. **NIWA Client Report**, v. 123, Jan. 2006. Available from: <https://www.researchgate.net/publication/266409739_Application_of_Floating_Wetlands_for_Enhanced_Stormwater_Treatment_A_Review>. Cit. on pp. 3, 4, 7.

_____. Constructed Wetlands With Floating Emergent Macrophytes: An Innovative Stormwater Treatment Technology. **Critical Reviews in Environmental Science and Technology**, Taylor Francis, v. 42, n. 21, p. 2261–2310, 2012. DOI: 10.1080/10643389.2011.574108. Available from: <https://doi.org/10.1080/10643389.2011.574108>. Cit. on pp. 4, 5, 7, 26.

HOEGER, Sven. Schwimmkampen: Germany's artificial floating islands. **Journal of Soil and Water Conservation**, v. 43, n. 4, p. 304–306, 1988. ISSN 1941-3300. Cit. on p. 2.

KADLEC, Robert H.; WALLACE, Scott. **Treatment Wetlands**. [S.l.]: CRC Press, July 2008. DOI: 10.1201/9781420012514. Available from: <https://doi.org/10.1201/9781420012514>. Cit. on p. 37.

KEIZER-VLEK, Hanneke E. et al. The contribution of plant uptake to nutrient removal by floating treatment wetlands. **Ecological Engineering**, Elsevier BV, v. 73, p. 684–690, Dec. 2014. DOI: 10.1016/j.ecoleng.2014.09.081. Available from: <https://doi.org/10.1016/j.ecoleng.2014.09.081>. Cit. on p. 38.

KHAN, Sher. **Hydrodynamics of Sediment Retention Ponds**. 2012. PhD thesis – Dept. of Civil and Environmental Engineering, University of Auckland, Auckland, New Zealand. Cit. on pp. 4, 9, 15, 39.

KHAN, Sher; MELVILLE, Bruce W.; SHAMSELDIN, Asaad. Design of Storm-Water Retention Ponds with Floating Treatment Wetlands. **Journal of Environmental Engineering**, v. 139, n. 11, p. 1343–1349, 2013. DOI: 10.1061/(ASCE)EE.1943-7870.0000748. Available from: <https://ascelibrary.org/doi/10.1061/%28ASCE%29EE.1943-7870.0000748>. Cit. on pp. 4, 7, 8, 15, 24, 27, 38, 39.

KHAN, Sher; MELVILLE, Bruce W.; SHAMSELDIN, Asaad Y.; FISCHER, Christoph. Investigation of Flow Patterns in Storm Water Retention Ponds using CFD. **Journal of Environmental Engineering**, v. 139, n. 1, p. 61–69, 2013. DOI: 10.1061/(ASCE)EE.1943-7870.0000540. eprint: https://ascelibrary.org/doi/pdf/10.1061/%28ASCE%29EE.1943-7870.0000540. Cit. on p. 8.

KHAN, Sher; SHOAIB, Muhammad, et al. Hydraulic investigation of the impact of retrofitting floating treatment wetlands in retention ponds. **Water Science and Technology**, v. 80, n. 8, p. 1476–1484, 2019. DOI: 10.2166/wst.2019.397. Available from: <https://doi.org/10.2166/wst.2019.397>. Cit. on pp. 4, 5, 8, 37–39, 45.

LADISLAS, S. et al. Performances of Two Macrophytes Species in Floating Treatment Wetlands for Cadmium, Nickel, and Zinc Removal from Urban Stormwater Runoff. **Water, Air, & Soil Pollution**, Springer Science and Business Media LLC, v. 224, n. 2, Jan. 2013. DOI: 10.1007/s11270-012-1408-x. Available from: <https://doi.org/10.1007/s11270-012-1408-x>. Cit. on pp. 8, 38.

LU, Hsiao-Ling; KU, Chen-Ruei; CHANG, Yuan-Hsiou. Water quality improvement with artificial floating islands. **Ecological Engineering**, Elsevier BV, v. 74, p. 371–375, Jan. 2015. DOI: 10.1016/j.ecoleng.2014.11.013. Available from: <https://doi.org/10.1016/j.ecoleng.2014.11.013>. Cit. on p. 38.

LUCKE, T.; WALKER, C.; BEECHAM, S. Experimental designs of field-based constructed floating wetland studies: A review. **Science of The Total Environment**, v. 660, p. 199–208, 2019. DOI: https://doi.org/10.1016/j.scitotenv.2019.01.018. Available from: <https://www.sciencedirect.com/science/article/pii/S0048969719300191>. Cit. on p. 4.

LUO, Kun et al. Impacts of rapid urbanization on the water quality and macroinvertebrate communities of streams: A case study in Liangjiang New Area, China. **Science of the Total Environment**, v. 121, p. 1601–1614, 2017. DOI: 10.1016/j.scitotenv.2017.10.068. Available from: <https://doi.org/10.1016/j.scitotenv.2017.10.068>. Cit. on p. 1.

MACHADO XAVIER, Manoel Lucas; JANZEN, Johannes Gerson; NEPF, Heidi. Numerical modeling study to compare the nutrient removal potential of different floating treatment island configurations in a stormwater pond. **Ecological Engineering**, v. 111, p. 78–84, 2018. DOI: https://doi.org/10.1016/j.ecoleng.2017.11.022. Available from: <https://www.sciencedirect.com/science/article/pii/S092585741730633X>. Cit. on pp. 4, 5, 8–10, 15, 17, 18, 21–26, 38, 39, 41, 42.

MARSALEK, J.; MARSALEK, P.M. Characteristics of sediments from a stormwater management pond. **Water Science and Technology**, v. 36, n. 8, p. 117–122, 1997. DOI: https://doi.org/10.1016/S0273-1223(97)00610-0. Available from: <https://www.sciencedirect.com/science/article/pii/S0273122397006100>. Cit. on p. 3.

MENTER, F. R.; KUNTZ, M.; LANGTRY, R. Ten Years of Industrial Experience with the SST Turbulence Model. **Turbulence, Heat and Mass Transfer 4**, v. 1, p. 625–632, 2003. DOI: 10.1.1.460.2814. Cit. on pp. 12, 14, 41.

NAKAMURA, K.; MUELLER, G. Review of the Performance of the Artificial Floating Island as a Restoration Tool for Aquatic Environments. In: WORLD ENVIRONMENTAL AND WATER RESOURCES CONGRESS 2008, Ahupua'a. American Society of Civil Engineers. DOI: 10.1061/40976(316)276. Available from: <https://ascelibrary.org/doi/10.1061/40976%28316%29276>. Cit. on pp. 4, 37.

OUYANG, Tingping; ZHU, Zhaoyu; KUANG, Yaoqiu. title. **Environmental Monitoring and Assessment**, v. 120, p. 313–325, 2006. DOI: 10.1007/s10661-005-9064-x. Available from: <https://link.springer.com/article/10.1007/s10661-005-9064-x>. Cit. on p. 1.

PAVAN, Francesca; BRESCHIGLIARO, Simone; BORIN, Maurizio. Screening of 18 species for digestate phytodepuration. **Environmental Science and Pollution Research**, v. 22, p. 2455–2466, 2015. DOI: 10.1007/s11356-014-3247-3. Available from: <https://link.springer.com/article/10.1007/s11356-014-3247-3>. Cit. on p. 3.

PAVLINERI, Natalia; SKOULIKIDIS, Nikolaos Th.; TSIHRINTZIS, Vassilios A. Constructed Floating Wetlands: A review of research, design, operation and management aspects, and data meta-analysis. **Chemical Engineering Journal**, v. 308, p. 1120–1132, 2017. DOI: https://doi.org/10.1016/j.cej.2016.09.140. Available from: <https://www.sciencedirect.com/science/article/pii/S1385894716313857>. Cit. on pp. 2, 3, 8, 38.

PERSSON, J. The hydraulic performance of ponds of various layouts. **Urban Water**, v. 2, n. 3, p. 243–250, 2000. DOI: https://doi.org/10.1016/S1462-0758(00)00059-5. Available from: <https://www.sciencedirect.com/science/article/pii/S1462075800000595>. Cit. on pp. 4, 7.

POMPEU, Paulo S.; ALVES, Carlos Bernardo M.; CALLISTO, Marcos. The effects of urbanization on biodiversity and water quality in the Rio das Velhas basin, Brazil. In: AMERICAN Fisheries Society Symposium. [S.l.: s.n.], 2005. p. 11–22. Available from: <https://www.researchgate.net/publication/254956605_The_Effects_of_Urbanization_on_Biodiversity_and_Water_Quality_in_the_Rio_das_Velhas_Basin_Brazil>. Cit. on p. 1.

REN, Lijun; CUI, Erqian; SUN, Haoyu. Temporal and spatial variations in the relationship between urbanization and water quality. **Environmental Science and Pollution Research**, v. 21, n. 23, p. 13646–13655, 2014. DOI: 10.1007/s11356-014-3242-8. Available from: <https://link.springer.com/article/10.1007/s11356-014-3242-8>. Cit. on p. 1.

ROMINGER, JEFFREY T.; NEPF, HEIDI M. Flow adjustment and interior flow associated with a rectangular porous obstruction. **Journal of Fluid Mechanics**, Cambridge University Press (CUP), v. 680, p. 636–659, June 2011. DOI: 10.1017/jfm.2011.199. Available from: <https://doi.org/10.1017/jfm.2011.199>. Cit. on p. 23.

SABOKROUHIYEH, Nima et al. A numerical study of the effect of wetland shape and inlet-outlet configuration on wetland performance. **Ecological Engineering**, v. 105, p. 170–179, 2017. ISSN 0925-8574. DOI: https://doi.org/10.1016/j.ecoleng.2017.04.062. Available from:

<https://www.sciencedirect.com/science/article/pii/S0925857417302471>. Cit. on p. 21.

SONG, Hai-Liang et al. Investigation of microcystin removal from eutrophic surface water by aquatic vegetable bed. **Ecological Engineering**, v. 35, n. 11, p. 1589–1598, 2009. DOI: https://doi.org/10.1016/j.ecoleng.2008.04.005. Available from: <https://www.sciencedirect.com/science/article/pii/S0925857408000803>. Cit. on p. 4.

SRINIVASAN, Veena et al. The impact of urbanization on water vulnerability: A coupled human– environment system approach for Chennai, India. **Global Environmental Change**, v. 23, n. 1, p. 229–239, 2013. DOI: 10.1016/j.gloenvcha.2012.10.002. Available from: <https://doi.org/10.1016/j.gloenvcha.2012.10.002>. Cit. on p. 1.

STOTTMEISTER, U. et al. Effects of plants and microorganisms in constructed wetlands for wastewater treatment. **Biotechnology Advances**, v. 22, n. 1, p. 93–117, 2003. VI International Symposium on Environmental Biotechnology. DOI: https://doi.org/10.1016/j.biotechadv.2003.08.010. Available from: <https://www.sciencedirect.com/science/article/pii/S0734975003001319>. Cit. on p. 2.

SUSTAINABLE DEVELOPMENT, International Institute for. **Floating Treatment Wetlands**. 2018. Available from: <https://www.iisd.org/projects/floating-treatment-wetlands>. Visited on: 19 May 2021. Cit. on p. 2.

TANNER, Chris C.; HEADLEY, Tom R. Components of floating emergent macrophyte treatment wetlands influencing removal of stormwater pollutants. **Ecological Engineering**, Elsevier BV, v. 37, n. 3, p. 474–486, Mar. 2011. DOI: 10.1016/j.ecoleng.2010.12.012. Available from: <https://doi.org/10.1016/j.ecoleng.2010.12.012>. Cit. on pp. 37, 38, 45.

TROITSKY, Brendan et al. Nutrient processes and modeling in urban stormwater ponds and constructed wetlands. **Canadian Water Resources Journal / Revue canadienne des ressources hydriques**, Informa UK Limited, v. 44, n. 3, p. 230–247, Apr. 2019. DOI: 10.1080/07011784.2019.1594390. Available from: <https://doi.org/10.1080/07011784.2019.1594390>. Cit. on p. 38.

VYMAZAL, Jan. Constructed Wetlands for Wastewater Treatment: Five Decades of Experience. **Environmental Science Technology**, v. 45, n. 1, p. 61–69, 2011. DOI: 10.1021/es101403q. Available from: <https://pubs.acs.org/doi/10.1021/es101403q>. Cit. on p. 2.

VYMAZAL, Jan. Removal of nutrients in various types of constructed wetlands. **Science of The Total Environment**, v. 380, n. 1, p. 48–65, 2007. DOI: https://doi.org/10.1016/j.scitotenv.2006.09.014. Available from: <https://www.sciencedirect.com/science/article/pii/S0048969706007212>. Cit. on pp. 2, 8.

VYMAZAL, Jan et al. Removal mechanisms and types of constructed wetlands. In: **Constructed Wetlands for Wastewater Treatment in Europe**. Ed. by J. Vymazal. [S.l.]: Backhuys Publishers, Jan. 1998. p. 17–66. Leiden, The Netherlands. Cit. on p. 2.

WALKER, David J. Modelling residence time in stormwater ponds. **Ecological Engineering**, v. 10, n. 3, p. 247–262, 1998. DOI: https://doi.org/10.1016/S0925-8574(98)00016-0. Available from: <https://www.sciencedirect.com/science/article/pii/S0925857498000160>. Cit. on p. 3.

WANG, Wenjing et al. Urbanization Impacts on Natural Habitat and Ecosystem Services in the Guangdong-Hong Kong-Macao "Megacity". **Sustainability**, v. 12, n. 16, p. 1–17, 2020. DOI: doi:10.3390/su12166675. Available from: <https://www.mdpi.com/2071-1050/12/16/6675>. Cit. on p. 1.

WINSTON, Ryan J. et al. Evaluation of floating treatment wetlands as retrofits to existing stormwater retention ponds. **Ecological Engineering**, Elsevier BV, v. 54, p. 254–265, May 2013. DOI: 10.1016/j.ecoleng.2013.01.023. Available from: <https://doi.org/10.1016/j.ecoleng.2013.01.023>. Cit. on p. 38.

WU, Haiming et al. A review on the sustainability of constructed wetlands for wastewater treatment: Design and operation. **Bioresource Technology**, Elsevier BV, v. 175, p. 594–601, Jan. 2015. DOI: 10.1016/j.biortech.2014.10.068. Available from: <https://doi.org/10.1016/j.biortech.2014.10.068>. Cit. on p. 38.

YEH, Naichia; YEH, Pulin; CHANG, Yuan-Hsiou. Artificial floating islands for environmental improvement. **Renewable and Sustainable Energy Reviews**, v. 47, p. 616–622, 2015. DOI: https://doi.org/10.1016/j.rser.2015.03.090. Available from: <https://www.sciencedirect.com/science/article/pii/S1364032115002439>. Cit. on p. 2.

ZHANG, Chong-Bang et al. Comparison of effects of plant and biofilm bacterial community parameters on removal performances of pollutants in floating island systems. **Ecological Engineering**, v. 73, p. 58–63, 2014. DOI: https://doi.org/10.1016/j.ecoleng.2014.09.023. Available from: <https://www.sciencedirect.com/science/article/pii/S0925857414004212>. Cit. on p. 2.